THE ASTROPHYSICAL JOURNAL

AN INTERNATIONAL REVIEW OF SPECTROSCOPY AND ASTRONOMICAL PHYSICS

VOLUME 85 JUNE 1937 NUMBER 5

A DETERMINATION OF THE AMOUNT OF CARBON DIOXIDE ABOVE THE REFLECTING LAYER IN THE ATMOSPHERE OF THE PLANET VENUS

ARTHUR ADEL

ABSTRACT

Previous analysis has established the identity of the initial and final states of the three absorption bands photographed by W. S. Adams and T. Dunham, Jr., in the infrared spectrum of Venus and traced by them to the molecule of carbon dioxide. The present investigation concerns itself with the determination of the wave-functions of these states and the subsequent calculation of the transition intensities. These results are combined with the transition intensity of the fundamental absorption band ν_3, for which band the percentage absorption is known, approximately, as a function of the path length. It follows that an equivalent path length of approximately 400 m−atm of carbon dioxide is required to develop the absorption bands $5\nu_3$ and $5\nu_3 + \binom{\nu_1}{2\nu_2}$ as they appear in the spectrum of Venus. This estimate is probably low, in view of experiments performed by Dunham and by Adel and Slipher on the quantity of carbon dioxide required to duplicate the spectrum of Venus. However, because of the accuracy with which the constants entering the calculation are known, the computed result is probably better than the order of magnitude.

I. INTRODUCTION

It is now well known that the molecule of carbon dioxide possesses a form which is both linear and symmetrical, the carbon atom lying midway between the two oxygens.[1] The group of normal vibrations of such a system constitute an approximate solution of zero order for the motion, which very satisfactorily explains the general features of the infrared spectrum of the molecule. The respective modes of vibration of the three independent frequencies are indicated schematically in Figure 1.

[1] A. Adel and D. M. Dennison, *Phys. Rev.*, **43**, 716; **44**, 99, 1933.

The first of these, ω_1, corresponds to a symmetrical motion of the oxygen atoms, the carbon atom remaining fixed at the center of mass. This frequency is inactive in the infrared but will appear strongly in the Raman spectrum and lies at about 7.5μ. In the second frequency, ω_2, the carbon oscillates perpendicularly to the line joining the oxygen atoms, while the distance between the oxygens remains unchanged. ω_2 is a double frequency, active in the infrared, inactive in the Raman spectrum, and lies at about 15μ. The unsymmetrical vibration with frequency, ω_3, is a motion of the

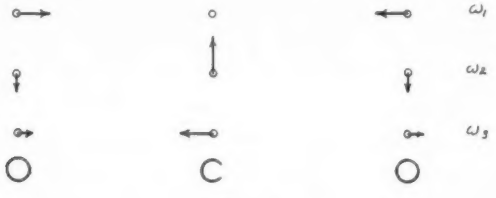

FIG. 1

atoms along the figure axis of the molecule in which the carbon moves relative to the center of mass of the oxygens, where again the distance between the latter remains unaltered during the motion. This frequency, which is active in the infrared and inactive in the Raman spectrum, lies at about 4.7μ.

As has been remarked above, this model fully explains the principal observed features of the spectrum. When, however, the infrared and Raman spectra are examined more carefully, certain details appear which cannot be so simply understood. The Raman spectrum, for example, consists not of one, but of two, lines of about equal intensity in the region of about 7.5μ. Moreover, many of the combination bands in the infrared deviate from the positions predicted by the combination relations by rather large amounts (i.e., approximately 100 cm^{-1}).

These difficulties have been traced by Fermi[2] to the circumstance that in carbon dioxide the frequency, ω_1, is almost exactly equal to $2\ \omega_2$. The degeneracy thus introduced requires a first-order perturbation for its resolution. This perturbation alters the identity of the levels, allowing two Raman lines rather than one to appear. It

[2] *Zt. f. Phys.* **71**, 250, 1931.

exercises also a profound effect upon the appearance of the spectrum of Venus by conditioning the relative intensity of the absorption bands $5\nu_3 + \begin{pmatrix} \nu_1 \\ 2\nu_2 \end{pmatrix}$. The perturbation yields a first-order correction to the zero-order energy, which accounts roughly for the positions of the combination bands. Adel and Dennison[1] have taken into account all the various perturbing forces in the motions of the carbon dioxide molecule and have applied them in both the first and the second orders, thereby achieving excellent agreement between theory and experiment. The positions of the observed lines can be forecast with an error not in excess of the experimental one; that is, one or two cm^{-1}. The positional features of the infrared and Raman spectra of the carbon dioxide molecule have now been completely accounted for. Similar treatment has not yet been accorded the problem of intensity relationships within the observable spectrum. It is proposed in this paper to investigate this phase of the problem in its relation to the carbon dioxide absorption bands in the spectrum of Venus.

II. ANALYSIS

In presenting the analysis we shall use the co-ordinates q, z, r, and φ, which were first introduced by Dennison[3] in the discussion of the molecule YX_2. q measures the relative separation of the oxygen atoms; z, the displacement of the carbon atom from the center of mass of the oxygens, measured parallel to the line of the latter; while r and φ are the polar co-ordinates of the carbon atom in a plane at right angles to the line of the oxygens, the origin of the co-ordinates lying at the intersection.

It is convenient to introduce the dimensionless variables σ, ξ, ρ, and φ instead of q, z, r, and φ, which are related to them in the following manner:

$$\sigma = \left\{\frac{2\pi^2\omega_1 m}{h}\right\}^{\frac{1}{2}} q \qquad \xi = \left\{\frac{4\pi^2\omega_3\mu}{h}\right\}^{\frac{1}{2}} z$$

$$\rho = \left\{\frac{4\pi^2\omega_2\mu}{h}\right\}^{\frac{1}{2}} r \qquad \varphi = \varphi$$

[3] *Rev. Mod. Phys.* **3**, 280, 1931.

where h is Planck's constant; m is the mass of an oxygen atom; and $\mu = 2mM/(2m + M)$, M being the mass of the carbon atom. One may describe $m/2$ as the reduced mass associated with the vibration ω_1, and μ as the reduced mass associated with the vibrations ω_2 and ω_3.

The Hamiltonian representing the vibrational motion conforms to the symmetry of the molecule and may be expressed, correct through the second-order approximation, as[1]

$$H \equiv H_0 + \lambda H_1 + \lambda^2 H_2 ,$$

$$H_0 \equiv \frac{2\pi^2}{h}\left\{ 2\omega_2 p_\sigma^2 + \omega_3 p_\xi^2 + \omega_2 p_\rho^2 + \frac{\omega_2}{\rho_2}\, p_\varphi^2 \right\} + \frac{h}{2}\left\{ 2\omega_2\sigma^2 + \omega_2\rho^2 + \omega_3\xi^2 \right\} ,$$

$$\lambda H_1 \equiv \frac{2\pi^2\Delta}{h}\, p_\sigma^2 + h\left\{ \frac{\Delta}{2}\,\sigma^2 + a\sigma^3 + b\sigma\rho^2 + c\sigma\xi^2 \right\} ,$$

$$\lambda^2 H_2 \equiv \frac{\omega_3}{2\omega_2 I}\,\rho^2 p_\xi^2 + h\left\{ d\sigma^4 + e\rho^4 + f\xi^4 + g\sigma^2\rho^2 + h\sigma^2\xi^2 + i\rho^2\xi^2 \right\} .$$

The zero-order portion, H_0, assumes that the oscillations are simple harmonic and that $\omega_1 = 2\omega_2$. The p's are, of course, the generalized momenta. The first-order portion, λH_1, is to be considered as a first-order perturbation potential and is composed of two classes of terms. The first class represents the fact that ω_1 is not precisely twice ω_2, the difference being $\Delta = \omega_1 - 2\omega_2$; while the second class is composed of the terms which mark the first-order deviation from simple harmonic motion, namely, the cubic anharmonic potential. The second-order portion, $\lambda^2 H_2$, may likewise be divided into two parts. The first of these, $(\omega_3/2\omega_2 I)\rho^2 p_\xi^2$, embodies the circumstance that, for finite amplitudes of vibration, the form of the molecule deviates slightly from strict linearity. The second part is composed of the terms which mark the second-order deviation from simple harmonic motion, namely, the quartic anharmonic potential. The analysis, as will become evident, must be developed at least through the second-order correction, $\lambda^2 H_2$, to permit the transitions, $5\nu_3 + \binom{\nu_1}{2\nu_2}$, observed in the spectrum of Venus. The absorption band $5\nu_3$, also observed in the spectrum of Venus, requires the application of only the first-order perturbation potential λH_1. It will be noted

that the ω's are employed to represent the simple harmonic frequencies of the zero-order approximate solution, whereas the ν's are used to denote the actual, fully corrected (and therefore observed) anharmonic frequencies.

From the zero-order Hamiltonian the wave-equation of the vibrating molecule is set up in the usual manner. The wave-functions satisfying this differential equation and fulfilling the boundary conditions may be expressed in the form

$$ {}_0\Psi^{V_1 V_2 l V_3} = \Psi^{V_1}_{(\sigma)} \Psi^{V_3}_{(\xi)} R^{V_2 l}_{(\rho)} e^{\pm i l \varphi} . $$

V_1, (V_2, l), and V_3 are the quantum numbers associated with the vibrations, ω_1, ω_2, and ω_3, respectively. $\Psi^{V_1}_{(\sigma)}$ and $\Psi^{V_3}_{(\xi)}$ are the well-known Hermitian orthogonal functions which, in normalized form, have the appearance, respectively:

$$ \Psi^{V_1}_{(\sigma)} = \{ 2^{V_1} V_1 ! \sqrt{\pi} \}^{-\frac{1}{2}} H^{V_1}_{(\sigma)} e^{-\frac{\sigma^2}{2}} $$

$$ \Psi^{V_3}_{(\xi)} = \{ 2^{V_3} V_3 ! \sqrt{\pi} \}^{-\frac{1}{2}} H^{V_3}_{(\xi)} e^{-\frac{\xi^2}{2}} , $$

where $H^{V_1}_{(\sigma)}$ is the V_1th order Hermitian polynomial of argument σ and is generated by means of the expression

$$ \sum_{V_1 = 0}^{\infty} \frac{t^{V_1}}{V_1 !} e^{-\frac{\sigma^2}{2}} H^{V_1}_{(\sigma)} = e^{\left(-t^2 + 2t\sigma - \frac{\sigma^2}{2} \right)} ; $$

and similarly for $H^{V_3}_{(\xi)}$. On the other hand, $R^{V_2 l}_{(\rho)} e^{\pm i l \varphi}$ is given in normalized form by

$$ (k!)^{\frac{1}{2}} \{ (l + k)! \}^{-\frac{1}{2}} \pi^{-\frac{1}{2}} \rho^l e^{-\frac{\rho^2}{2}} L^l_{(l+k)}(\rho^2) e^{\pm i l \varphi} , $$

where $k = (V_2 - l)/2$. $L^l_{(l+k)}(\rho^2)$ is the associated Laguerre polynomial of argument, ρ^2, and is generated by means of the expression

$$ \sum_{k=0}^{\infty} L^l_{(l+k)}(\rho^2) \frac{t^k}{(l + k)!} = (-1)^l \frac{e^{-\frac{\rho^2 t}{1-t}}}{(1 - t)^{l+1}} . $$

$$ \Psi^{V_2 l}_{(\rho, \varphi)} = R^{V_2 l}_{(\rho)} e^{\pm i l \varphi} $$

obviously represents the motion of a simple harmonic oscillator in a plane, while $\Psi_{(\sigma)}^{V_1}$ and $\Psi_{(\xi)}^{V_3}$ represent simple harmonic oscillators on a line. The zero-order energy of vibration is given by

$$_0E = h\{\omega_1(V_1 + \tfrac{1}{2}) + \omega_2(V_2 + 1) + \omega_3(V_3 + \tfrac{1}{2})\},$$

or

$$_0E = h\{\omega_2(2V_1 + V_2 + 1) + \omega_3(V_3 + \tfrac{1}{2})\},$$

since $\omega_1 = 2\omega_2$.

A transition from one vibrational state to another by the absorption of a quantum of radiation is permitted when the matrix element of the electric moment of the molecule is nonvanishing between the two states in question. The component of the electric moment along the figure axis is $\alpha\xi$, and the component perpendicular to the figure axis is $\beta\rho e^{i\varphi}$, where α and β are constant coefficients. It is well known that, to a zero-order approximation, only certain fundamental transitions are permitted and that no harmonic or combination bands may appear. The electric moment cannot be altered to make the higher transitions possible, but the wave-functions must be corrected by application of the cubic and quartic anharmonic perturbation potentials.

Let us consider first the transition

$$\begin{array}{ll} V_1\ 0 \to 0 & l\ \ 0 \to 0 \\ V_2\ 0 \to 0 & V_3\ 0 \to 5 \end{array}$$

This transition produces the Venus band $5\nu_3$ with its center at 11469.5 cm^{-1}. The initial and final states of the transition are nondegenerate, there being but one wave-function per level; and hence the wave-functions may be corrected by means of the customary perturbation theory of nondegenerate systems. Turning to the transitions

$$\begin{array}{ll} V_1\ 0 \to & \\ V_2\ 0 \to & \begin{pmatrix} 1 \\ 0 \\ 0 \\ 5 \end{pmatrix} \begin{pmatrix} 0 \\ 2 \\ 0 \\ 5 \end{pmatrix} \\ l\ \ 0 \to & \\ V_3\ 0 \to & \end{array}$$

which produce the Venus bands $5\nu_3 + \begin{pmatrix} \nu_1 \\ 2\nu_2 \end{pmatrix}$, with centers at 12672.4 cm^{-1} and 12774.7 cm^{-1}, we find that the problem of correcting the wave-functions is somewhat more elaborate. In the zero-order approximate solution set forth above we found that these two upper states are coincident and are, therefore, degenerate. Consequently, before the wave-functions for these excited states may be corrected by the perturbation mechanism for nondegenerate systems, the inherent degeneracy must be removed. To resolve the degeneracy, the secular determinental equation is established, namely,

$$\left| (\lambda H_1)^{nt''}_{nt'} - (\lambda E_1)^{n\tau} \delta^{t''}_{t'} \right| = 0 ,$$

where n represents the quantum numbers $2V_1 + V_2$, V_3; and t represents the quantum numbers of which ${}_0E$ is independent, namely, V_1, V_2, and l. $\delta^{t''}_{t'} = 1$ when $t' = t''$ and is zero when $t' \neq t''$. The index τ serves to enumerate the levels as they are separated by the perturbation. The energies of the resolved levels are obtained by adding

$$(\lambda E_1)^{n\tau_1} = h\left\{\Delta + \left[\frac{\Delta^2}{4} + \frac{b^2}{2}\right]^{\frac{1}{2}}\right\}$$

to the zero-order energy to form the upper level and by adding

$$(\lambda E_1)^{n\tau_2} = h\left\{\Delta - \left[\frac{\Delta^2}{4} + \frac{b^2}{2}\right]^{\frac{1}{2}}\right\}$$

to the zero-order energy to form the lower level. The appropriate stabilized wave-functions for these new levels are the properly chosen linear combinations

$$\Psi^{n\tau} = \sum_t C_{\tau t} \Psi^{nt} ,$$

where the $C_{\tau t}$ are given by the first minors of the secular determinant for $(\lambda E_1)^{n\tau}$.

The degeneracy has been removed. The proper zero-order wave-functions involved in the transitions appearing in the spectrum of Venus have been established, and we may proceed with their correc-

tion as conditioned by the first- and second-order corrections to the potential function. Figure 2 shows the zero-order vibrational energy-level diagram and the appropriate zero-order wave-functions.

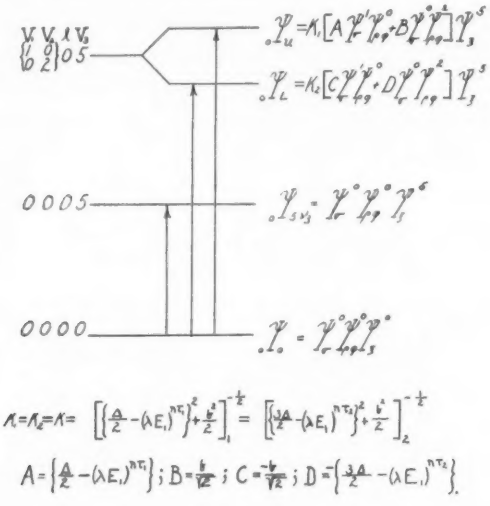

FIG. 2

It will be sufficient to treat $\lambda H_1 + \lambda^2 H_2$ as a single perturbation λV. The corrected wave-functions are then given by

$$\Psi^k = {}_0\Psi^k + \sum_{j=0}^{\infty}{}' \frac{\int_\tau {}_0\Psi^j(\lambda V)_0\Psi^k \, d\tau}{{}_0E_k - {}_0E_j} \cdot {}_0\Psi^j ,$$

where the prime denotes the omission of the term $j = k$. In the following analysis it will be convenient to represent

$$\Psi^{V_1}_{(\sigma)}\Psi^{V_2 O}_{(\rho,\varphi)}\Psi^{V_3}_{(\xi)}$$

by the symbol $(V_1V_2V_3)$. The term $\Delta\,(V_1 + \frac{1}{2})$ does not contribute. Furthermore, the first part of $\lambda^2 H_2$ may be neglected because of quantitative smallness. We find that the following wave-functions in Table 1 possess nonvanishing coefficients and are therefore contributed as corrections.

TABLE 1

CORRECTIONS TO THE WAVE-FUNCTION OF THE GROUND STATE

By	Correction Terms
$a\sigma^3$	(100), (300)
$b\sigma\rho^2$	(100), (120)
$c\sigma\xi^2$	(100), (102)
$d\sigma^4$	(200), (400)
$e\rho^4$	(020), (040)
$f\xi^4$	(002), (004)
$g\sigma^2\rho^2$	(020), (200), (220)
$h\sigma^2\xi^2$	(002), (200), (202)
$i\rho^2\xi^2$	(002), (020), (022)

CORRECTIONS TO THE WAVE-FUNCTION OF THE EXCITED STATE $5\nu_3$

By	Correction Terms
$a\sigma^3$	(105), (305)
$b\sigma\rho^2$	(105), (125)
$c\sigma\xi^2$	(103), (105), (107)
$d\sigma^4$	(205), (405)
$e\rho^4$	(025), (045)
$f\xi^4$	(001), (003), (007), (009)
$g\sigma^2\rho^2$	(025), (225), (205)
$h\sigma^2\xi^2$	(003), (007), (203), (205), (207)
$i\rho^2\xi^2$	(003), (007), (023), (025), (027)

CORRECTIONS TO THE WAVE-FUNCTION OF THE EXCITED STATE $\left\{5\nu_3 + \binom{\nu_1}{2\nu_2}\right\}_U$

By	Correction Terms
$a\sigma^3$	(005), (205), (405), (125), (325)
$c\sigma\xi^2$	(003), (007), (005), (205), (203), (207), (125), (123), (127)
$d\sigma^4$	(305), (505), (225), (425)
$e\rho^4$	(125), (145), (005), (045), (065)
$f\xi^4$	(101), (103), (107), (109), (021), (023), (027), (029)
$g\sigma^2\rho^2$	(125), (325), (305), (005), (045), (205), (225), (245)
$h\sigma^2\xi^2$	(103), (107), (305), (303), (307), (023), (027), (225), (223), (227)
$i\rho^2\xi^2$	(103), (107), (125), (123), (127), (005), (003), (007), (045), (043), (047), (023), (027)

CORRECTIONS TO THE WAVE-FUNCTION OF THE EXCITED STATE $\left\{5\nu_3 + \binom{\nu_1}{2\nu_2}\right\}_L$

The same correction terms appear here as appear in the expression for the corrected wave-function for the excited state $\left\{5\nu^3 + \binom{\nu_1}{2\nu_2}\right\}_U$, but with modified coefficients.

The term $b\sigma\rho^2$ has not been applied in correcting the wave-functions of the excited states, $5\nu_3 + \begin{pmatrix} \nu_1 \\ 2\nu_2 \end{pmatrix}$, apropos of its having been previously employed to remove the resonance degeneracy.

An examination of the correction terms in conjunction with the electric moment reveals that not all of them contribute to the matrix element of the electric moment. In the transition $0 \to 5\nu_3$, for example, it becomes evident that the component of electric moment $\beta\rho e^{i\varphi}$ is ineffective. The effective electric moment is therefore $a\xi$. Hence, only those pairs of terms (a pair being composed of one term from the ground state and one from the state $5\nu_3$) will be significant which possess identical quantum numbers V_1, V_2, l and which differ in V_3 by unity. The effective wave-functions for the transition are consequently given by

THE GROUND STATE

$$\Psi_{gd} = (000) + \frac{\int_\tau (102) c\sigma\xi^2 (000) d\tau}{-(\omega_1 + 2\omega_3)} (102) + \frac{\int_\tau (002) f\xi^4 (000) d\tau}{-2\omega_3} (002)$$
$$+ \frac{\int_\tau (004) f\xi^4 (000) d\tau}{-4\omega_3} (004) + \frac{\int_\tau (002) h\sigma^2\xi^2 (000) d\tau}{-2\omega_3} (002)$$
$$+ \frac{\int_\tau (002) i\rho^2\xi^2 (000) d\tau}{-2\omega_3} (002)$$

THE EXCITED STATE $5\nu^3$

$$\Psi_{5\nu_3} = (005) + \frac{\int_\tau (103) c\sigma\xi^2 (005) d\tau}{2\omega_3 - \omega_1} (103) + \frac{\int_\tau (001) f\xi^4 (005) d\tau}{4\omega_3} (001)$$
$$+ \frac{\int_\tau (003) f\xi^4 (005) d\tau}{2\omega_3} (003) + \frac{\int_\tau (003) h\sigma^2\xi^2 (005) d\tau}{2\omega_3} (003)$$
$$+ \frac{\int_\tau (003) i\rho^2\xi^2 (005) d\tau}{2\omega_3} (003) .$$

Since

$$\int_\tau d\tau \equiv \int_0^{2\pi}\int_0^{\infty}\int_{-\infty}^{\infty}\int_{-\infty}^{\infty} d\sigma\, d\xi\, d\rho\, \rho d\varphi\ ,$$

we have, upon carrying out the integrations:

$$\Psi_{gd} = (000) + \frac{c}{-\,2(\omega_1 + 2\omega_3)}(102) + \frac{\sqrt{\tfrac{3}{2}}f}{-\,4\omega_3}(004) + \frac{\tfrac{1}{2}h + i + \tfrac{3}{4}f}{-\,2\sqrt{2}\,\omega_3}(002)\ .$$

$$\Psi_{5\nu_3} = (005) + \frac{\sqrt{10}\,c}{2(2\omega_3 - \omega_1)}(103) + \frac{\sqrt{\tfrac{15}{2}}f}{4\omega_3}(001) + \frac{\tfrac{1}{2}\sqrt{5}\,h + \sqrt{5}\,i + \tfrac{3}{8}\sqrt{5}f}{2\omega_3}(003)\ .$$

For the transitions $0 \to 5\nu_3 + \begin{pmatrix}\nu_1\\ 2\nu_2\end{pmatrix}$, the effective correction terms are again determined by considering pairs of terms in the light of the electric moment. Since the correction terms both in the wave-function for the ground state and in the wave-functions for the upper states are even in the quantum number V_2, the component of electric moment $\beta\rho e^{i\varphi}$ may be neglected, for

$$\int_0^{2\pi} e^{i\varphi}\cdot e^{\pm 2in\varphi}d\varphi = 0\ .$$

We may again confine our attention to $a\xi$. And again only those pairs of terms which are identical in V_1 and V_2 and which differ by unity in V_3 are effective. It follows that the effective wave-functions are given by the expressions

$$\Psi_{gd} = -\frac{\tfrac{3}{2}\sqrt{\tfrac{1}{2}}\,a + \sqrt{\tfrac{1}{2}}\,b + \tfrac{1}{2}\sqrt{\tfrac{1}{2}}\,c}{\omega_1}(100) - \frac{\dfrac{3}{4\sqrt{2}}f + \dfrac{1}{2\sqrt{2}}h + \dfrac{1}{\sqrt{2}}i}{2\omega_3}(002) - \frac{\sqrt{\tfrac{1}{2}}\,c}{\omega_1 + 2\omega_3}(102) - \frac{\sqrt{\tfrac{3}{2}}f}{4\omega_3}(004)\ .$$

$$\Psi_{\left\{5\nu_3+\binom{\nu_1}{2\nu_2}\right\}_U} = \frac{U\left\{\frac{3}{2\sqrt{2}}a + \frac{11}{2\sqrt{2}}c\right\}}{E_U - 5\omega_3}(005) + \frac{U\frac{1}{2}\sqrt{10}\,c}{E_U - 3\omega_3}(003)$$
$$+ \frac{U\{\frac{3.7}{8}\sqrt{5}f + \frac{3}{2}\sqrt{5}h + \sqrt{5}i\}}{E_U - (\omega_1 + 3\omega_3)}(103) + \frac{U\sqrt{\frac{1.5}{2}}f}{E_U - (\omega_1 + \omega_3)}(101).$$

$$\Psi_{\left\{5\nu_3+\binom{\nu_1}{2\nu_2}\right\}_L} = \frac{L\left\{\frac{3}{2\sqrt{2}}a + \frac{11}{2\sqrt{2}}c\right\}}{E_L - 5\omega_3}(005) + \frac{L\frac{1}{2}\sqrt{10}\,c}{E_L - 3\omega_3}(003)$$
$$+ \frac{L\{\frac{3.7}{8}\sqrt{5}f + \frac{3}{2}\sqrt{5}h + \sqrt{5}i\}}{E_L - (\omega_1 + 3\omega_3)}(103) + \frac{L\sqrt{\frac{1.5}{2}}f}{E_L - (\omega_1 + \omega_3)}(101).$$

$$U = K\left(\frac{\Delta}{2} - [\lambda E_1]^{n\tau_1}\right); \qquad E_U = 2\omega_2 + 5\omega_3 + \frac{\Delta}{2} + \sqrt{\frac{\Delta^2}{4} + \frac{b^2}{2}}$$

$$L = K\frac{b}{\sqrt{2}}; \qquad E_L = 2\omega_2 + 5\omega_3 + \frac{\Delta}{2} - \sqrt{\frac{\Delta^2}{4} + \frac{b^2}{2}}.$$

It is necessary to determine the values of the coefficients $a \ldots . i$ which enter the expressions for the wave-functions. Through the application of the first- and second-order corrections to the vibrational energy-levels, Adel and Dennison[1] have derived the functional dependence of the energy upon these coefficients. They have further examined the interaction between rotation and vibration in the

TABLE 2

CONSTANTS OE THE POTENTIAL FUNCTION

$\omega_1 = 1361$	cm^{-1}	$a = -37$	cm^{-1}	$d = 6.6\,cm^{-1}$		$g = -9.9\,cm^{-1}$	
$\omega_2 = 673$		$b = 72.9$		$e = 2.0$		$h = 7.7$	
$\omega_3 = 2378$		$c = -202.1$		$f = 2.4$		$i = -12.3$	
$\Delta = 14.7$							

molecule and have shown how the magnitude of the interaction depends upon the first-order coefficients a, b, c. The effect of this interaction is a convergence and divergence of fine structure in the rotation-vibration bands. Observation of the latter provides additional equations in a, b, c. Employing all the relationships thus obtained, they have evaluated the coefficients. b and c (as well as ω_1, ω_2, ω_3)

are the most accurately known, with a probable error of about $\frac{1}{2}$ per cent. a is probably known to within 5 per cent, while the remaining constants may well be in error by as much as from 10 to 15 per cent. The values are listed in Table 2.

The effective corrected wave-functions can now be given explicitly:

FOR THE TRANSITION $0 \to 5\nu_3$

$$\Psi_{gd} = \Psi^{0}_{(\sigma)}\Psi^{0}_{(\xi)}\Psi^{0,0}_{(\rho,\varphi)} + 0.018\,\Psi^{1}_{(\sigma)}\Psi^{2}_{(\xi)}\Psi^{0,0}_{(\rho,\varphi)} - 0.0003\,\Psi^{0}_{(\sigma)}\Psi^{4}_{(\xi)}\Psi^{0,0}_{(\rho,\varphi)},$$

$$\Psi_{5\nu_3} = \Psi^{0}_{(\sigma)}\Psi^{5}_{(\xi)}\Psi^{0,0}_{(\rho,\varphi)} - 0.103\,\Psi^{1}_{(\sigma)}\Psi^{3}_{(\xi)}\Psi^{0,0}_{(\rho,\varphi)} + 0.0007\,\Psi^{0}_{(\sigma)}\Psi^{1}_{(\xi)}\Psi^{0,0}_{(\rho,\varphi)}.$$

FOR THE TRANSITIONS $0 \to 5\nu_3 + \binom{\nu_1}{2\nu_2}$

We shall assume here that $E_U \cong E_L$. The error committed in making this approximation has a negligible influence upon the results.

$$\Psi_{gd} = 0.028\,\Psi^{1}_{(\sigma)}\Psi^{0}_{(\xi)}\Psi^{0,0}_{(\rho,\varphi)} + 0.023\,\Psi^{1}_{(\sigma)}\Psi^{2}_{(\xi)}\Psi^{0,0}_{(\rho,\varphi)} + 0.001\,\Psi^{0}_{(\sigma)}\Psi^{2}_{(\xi)}\Psi^{0,0}_{(\rho,\varphi)} - 0.0003\,\Psi^{0}_{(\sigma)}\Psi^{4}_{(\xi)}\Psi^{0,0}_{(\rho,\varphi)},$$

$$\Psi_{\left\{5\nu_3+\binom{\nu_1}{2\nu_2}\right\}_U} = U\{-0.61\,\Psi^{0}_{(\sigma)}\Psi^{5}_{(\xi)}\Psi^{0,0}_{(\rho,\varphi)} - 0.052\,\Psi^{0}_{(\sigma)}\Psi^{3}_{(\xi)}\Psi^{0,0}_{(\rho,\varphi)} + 0.0049\,\Psi^{1}_{(\sigma)}\Psi^{3}_{(\xi)}\Psi^{0,0}_{(\rho,\varphi)} + 0.0007\,\Psi^{1}_{(\sigma)}\Psi^{1}_{(\xi)}\Psi^{0,0}_{(\rho,\varphi)}\},$$

$$\Psi_{\left\{5\nu_3+\binom{\nu_1}{2\nu_2}\right\}_L} = L\{-0.61\,\Psi^{0}_{(\sigma)}\Psi^{5}_{(\xi)}\Psi^{0,0}_{(\rho,\varphi)} - 0.052\,\Psi^{0}_{(\sigma)}\Psi^{3}_{(\xi)}\Psi^{0,0}_{(\rho,\varphi)} + 0.0049\,\Psi^{1}_{(\sigma)}\Psi^{3}_{(\xi)}\Psi^{0,0}_{(\rho,\varphi)} + 0.0007\,\Psi^{1}_{(\sigma)}\Psi^{1}_{(\xi)}\Psi^{0,0}_{(\rho,\varphi)}\}.$$

The matrix elements of the electric moment for the several transitions can now be obtained. We have

$$\epsilon_{0\to 5\nu_3} = \int_\tau \Psi_{gd}\,a\xi\,\Psi_{5\nu_3}\,d\tau = -2.3\times 10^{-3}a,$$

$$\epsilon_{0\to\left\{5\nu_3+\binom{\nu_1}{2\nu_2}\right\}_U} = \int_\tau \Psi_{gd}\,a\xi\,\Psi_{\left\{5\nu_3+\binom{\nu_1}{2\nu_2}\right\}_U}\,d\tau = 3.4\times 10^{-4}Ua,$$

$$\epsilon_{0\to\left\{5\nu_3+\binom{\nu_1}{2\nu_2}\right\}_L} = \int_\tau \Psi_{gd}\,a\xi\,\Psi_{\left\{5\nu_3+\binom{\nu_1}{2\nu_2}\right\}_L}\,d\tau = 3.4\times 10^{-4}La.$$

Dennison[1] has developed expressions for the theoretical intensity $I = \int_{\nu} a_{\nu} d\nu$, where a_{ν} is the true absorption coefficient of the gas. For the transitions in question these expressions reduce to

$$\swarrow^{j}_{j-1} I = A \frac{j}{4} e^{-\sigma(j^2+j)} \qquad \text{for a negative branch line,}$$

$$\swarrow^{j-1}_{j} I = A \frac{j}{4} e^{-\sigma(j^2-j)} \qquad \text{for a positive branch line.}$$

where j is the rotational quantum number, the energy of rotation being $(h^2/8\pi^2 I)j(j+1)$.

$$\sigma = \frac{h^2}{8\pi^2 I k T},$$

$$A = \frac{8\pi^3 \nu_0 N}{3ch \sum g_j e^{-\frac{Ej}{kT}}} \overline{\epsilon_{a\to b}}^2 \left(1 - e^{-\frac{h\nu_0}{kT}}\right),$$

where ν_0 is the frequency of the band center and N is the number of molecules per cubic centimeter in the ground state.

We observe that $e^{-\frac{h\nu_0}{kT}} \cong 0$ in virtue of the circumstance $h\nu_0 \ggg kT$. (The effective temperature for the absorbing layer of the atmosphere of Venus is approximately 250° absolute.) We may, consequently, write for the theoretical intensity of a given line of the band with its center at $I = \text{Const}\ \nu_0\ \overline{\epsilon_{a\to b}}^2$. For a given line in the bands of Venus, let us say the kth line of the negative branch, the theoretical intensities vary as

$$11496.5\ \overline{\epsilon_{0\to 5\nu_3}}^2 : 12672.4\ \overline{\epsilon_{0\to\left\{5\nu_3+\binom{\nu_1}{2\nu_2}\right\}_L}}^2 : 12774.7\ \overline{\epsilon_{0\to\left\{5\nu_3+\binom{\nu_1}{2\nu_2}\right\}_U}}^2.$$

Moreover, $U^2 \cong L^2 \cong \frac{1}{2}$. We may therefore consider the theoretical intensities of the kth lines in the negative branches of the bands $5\nu_3 + \binom{\nu_1}{2\nu_2}$ to be practically equal. Since

$$\frac{\overline{\epsilon_{0\to 5\nu_3}}^2}{\overline{\epsilon_{0\to\left\{5\nu_3+\binom{\nu_1}{2\nu_2}\right\}_{U \text{ or } L}}}^2} \cong 10^2,$$

and since

$$\frac{5\nu_3}{\left\{5\nu_3 + \binom{\nu_1}{2\nu_2}\right\}_{U \text{ or } L}} \cong 0.9 ,$$

it appears that

$$\left\{\frac{I_{5\nu_3}}{I_{\left\{5\nu_3+\binom{\nu_1}{2\nu_2}\right\}_{U \text{ or } L}}}\right\}_{k\text{th line}} \cong 90 .$$

In the same manner we may determine the relative theoretical intensities of the kth lines of the negative branches of the fundamental ν_3 and the Venus band $5\nu_3$. For $\epsilon_{0\to\nu_3}$ we have

$$\epsilon_{0\to\nu_3} = \int_\tau \Psi_{gd} a\xi \Psi_{\nu_3} d\tau = \frac{a}{\sqrt{2}} ,$$

and since $\nu_3 = 2350.1\ \text{cm}^{-1}$, we have

$$\left\{\frac{I_{\nu_3}}{I_{5\nu_3}}\right\}_{k\text{th line}} = 2 \times 10^4 .$$

The theoretical intensities are not directly observable quantities. However, one may observe the maximum percentage absorption in a line, to which the theoretical intensity is related. Dennison[4] has shown in his discussion of the *HCl* bands that to a good degree of approximation the true intensity and the observed minimum fractional transmission are connected by the expression

$$T_{\min} = e^{-\frac{2}{a}\sqrt{\frac{1.194N\sigma^2}{\sqrt{\pi hm}}}\cdot\sqrt{Il}} ,$$

where

$T_{\min}$ = Minimum fractional transmission
N = Number of molecules per cubic centimeter at standard pressure
σ = Distance to which two molecules may approach without altering each other's phases
a = Slit width of the spectrometer
h = $\frac{1}{2kT}$
m = Mass of a molecule
l = Path length of the gas

[4] *Phys. Rev.*, **31**, 503, 1928.

For the present need the salient feature of this expression is given by the relationship $T_{\min} = e^{-\text{cst}\sqrt{Il}}$.

It is now possible to form an approximate estimate of the quantity of carbon dioxide in the absorbing layer of the atmosphere of Venus. Adams and Dunham[5] have published photographic reproductions of the Venus bands $5\nu_3 + \binom{\nu_1}{2\nu_2}$, but none of $5\nu_3$. From an examination of the reproduced bands it seems probable that an assigned maximum absorption of 40 per cent for the seventh line[6] appearing in the negative branch of the shortest wave-band is a fair estimate—although the hazard inherent in judging transmissions from photographs must be borne in mind. The maximum absorption in the corresponding line of $5\nu_3$ can now be calculated from the relation

$$\{(T_{\min})_{5\nu_3}\}_{7\text{th line}} = \left\{(T_{\min})_{5\nu_3+\binom{\nu_1}{2\nu_2}}\right\}^{\sqrt{95}}_{7\text{th line}}.$$

It follows that the maximum absorption expected for the seventh line in the negative branch of $5\nu_3$ is approximately 99.3 per cent.

These results are now to be related to the observation by Martin and Barker[7] that the maximum absorption of the seventh line in the negative branch of ν_3 is 75 per cent, with an equivalent path of 0.15 cm − atm. of carbon dioxide[8] According to the relation $T_{\min} = e^{-\text{cst}\sqrt{Il}}$, the maximum absorption could be made to match that of the corresponding line in $5\nu_3$ in Venus by increasing the path length to kl, where $0.25^{\sqrt{k}} = 0.007$. Since $k = 13$, the required path length is approximately 2 cm/atm. It follows from $T_{\min} = e^{-\text{cst}\sqrt{Il}}$ that for a maximum absorption of 99.3 per cent in the seventh negative branch lines of ν_3 and $5\nu_3$, $(Il)_{\nu_3} = (Il)_{5\nu_3}$. Consequently,

[5] *Pub. A.S.P.*, **44**, 243, 1932.

[6] This is actually line No. 14, since alternate lines are completely forbidden by the selection rules.

[7] *Phys. Rev.*, **41**, 291, 1932.

[8] In applying the expressions containing N to the carbon dioxide in the atmosphere of Venus and to the carbon dioxide in the laboratory, we resort to the artifice of reducing all pressures to atmospheric pressures, thereby reducing N to a constant. The difference in the values of T for the upper layers of Venus and for the laboratory are neglected, since only minor errors result.

$l_{\text{Venus}} = 20{,}000 \times 2\text{ cm} - \text{atm} = 400\text{ m} - \text{atm}$. This is the equivalent path to and from the reflecting layer. The equivalent depth is therefore 200 m − atm. If we assume a maximum absorption of 20 per cent instead of 40 per cent for the seventh line appearing in the negative branch of $\left\{5\nu_3 + \begin{pmatrix}\nu_1\\ 2\nu_2\end{pmatrix}\right\}_U$, the equivalent path deduced for Venus is approximately 100 m − atm.

III. CONCLUSION

In experiments by Adel and Slipher[9] considerably more gas than this was required to show $5\nu_3$ in absorption. This was probably due to the blending of the fine structure by the pressure of approximately 50 atm to which the gas was subjected, thus spreading the absorption over a very broad, shallow region instead of confining it to sharp lines.

Dunham,[10] using the apparatus with which the bands of Venus were recorded, successfully observed $5\nu_3$ in the laboratory by using a path length of 400 m − atm (40 m at 10 atm), the laboratory band being weaker than the corresponding absorption in Venus. It is therefore clear that the result of our calculation is too small, but it is probably of the correct order of magnitude. This degree of agreement in a calculation of intensity of absorption is satisfactory.

LOWELL OBSERVATORY
FLAGSTAFF, ARIZONA
March 1937

[9] *Phys. Rev.*, **46**, 240, 1934.

[10] H. N. Russell, *Science*, **81**, January 4, 1935.

A COMPARISON OF THE RATES OF DEVELOPMENT OF NOVAE

DEAN B. McLAUGHLIN

ABSTRACT

Ann Arbor spectrograms and published data on the seven bright novae of the twentieth century furnish velocities of the *principal spectra* and the *diffuse enhanced spectra* and time intervals from maximum light to several distinctive spectroscopic phases of development. Those novae whose light faded slowly showed longer time intervals between spectroscopic phases and had lower absorption velocities. The magnitude drop from maximum to each spectroscopic phase is independent of the rate of development.

The seven novae were averaged by reducing them to a uniform time scale, through the intermediary of the light-curve. For all absorption-line stages there is a linear relation between the time of development of any nova and the time of development for the average of the seven.

If t is the time of development and r the rate, defined by the relation $r = 1/t$, it is found empirically that $r \sim V_1^2$ and $r \sim V_2^{5/2}$, where V_1 and V_2 are the velocities of the principal and the diffuse enhanced spectra, respectively. For the first appearance of the nebular radiations the rates are different, and the relation between the rates and the velocities is $r_n \sim V_1^{3/2}$.

Assuming that the state of the spectrum is determined by the density of ejected gases and the intensity of radiation from the central star, the exponents of V are of the expected order of magnitude. The similarity of novae, regardless of the rate of development, is emphasized.

It is well known that novae which decline more slowly in light also progress more slowly through their spectral changes and show smaller displacements of their absorption lines. Lack of a quantitative relation is probably due chiefly to two factors: (1) the lack of sufficiently detailed data on numerous individual novae and (2) the apparent complexity and uniqueness of each individual case for which extensive data are known.

The total number of objects for which sufficiently detailed information is available for comparison is seven, namely, the bright novae of the twentieth century. Even this statement is somewhat optimistic, for there are considerable gaps in our information about Nova Persei 1901. For five of these stars there are good series of spectrograms at the Observatory of the University of Michigan. These have been examined in detail by the writer, and extensive measures have been made of Nova Herculis. Sufficient measures have been made of Nova Aquilae and Nova Lacertae to outline the course of the changes. The plates of Nova Geminorum were supplemented by

reference to the work of Stratton[1] and of Wright.[2] In the case of Nova Cygni, the Ann Arbor material and some Mount Wilson plates have been studied in detail by R. B. Baldwin, and his investigation has been used as a source of information, supplemented by my own examination of the plates. For Nova Pictoris the extensive work of Jones[3] was referred to, and for Nova Persei the recent paper by Stratton[4] was used.

The study of rates of development is based on the recognition of a number of definite stages of the spectrum. Transitions involving the appearance or disappearance of certain features are especially useful; occasionally, maxima of development of certain lines can be used. The following broad stages and substages can be recognized in most well-observed novae:

1. *The pre-maximum stage.*—Three novae have shown a change from B to A type as they approached light-maximum. Two others, Nova Aquilae[5] and Nova Cygni, have shown change toward a later subdivision of class A during their rise, and it seems likely that they would have shown B-type spectra had they been observed soon enough. The remaining two (Nova Geminorum and Nova Pictoris) were caught too late to show such change.

2. Just after maximum light the emergence of the *principal absorption spectrum* and its associated emission bands furnishes a readily recognized stage.

3. A diffuse and more strongly displaced set of hydrogen and enhanced metallic lines appears a little later (one day or so in fast novae, weeks in slow ones). This will be referred to as the *diffuse enhanced spectrum*. Its emergence, maximum strength, and disappearance furnish three stages.

4. A set of Orion lines appears a few days later in rapid novae (months later in slow novae). Its appearance, maximum, and disappearance are three well-marked stages.

5. During the later absorption-line stages the hydrogen lines become conspicuously multiple during a relatively brief interval.

[1] *Ann. Solar Physics Obs., Cambridge*, **4**, 1, 1920.

[2] *Lick Obs. Pub.*, **14**, 27, 1926. [3] *Ann. Cape Obs.*, **10**, Part 9, 1931.

[4] *Ann. Solar Physics Obs., Cambridge*, **4**, 75, 1936.

[5] Parkhurst's slitless spectra, reproduced in *M.N.*, **79**, 498, 1919.

6. The well-known "4640 stage" is not so easy to fix accurately in time by its emission bands, since Orion emissions in that region may give rise to a pseudo-4640 stage. However, the appearance and disappearance of the *N* III absorptions λ 4097 and λ 4103 give two definite dates.

7. The nebular stage yields three recognizable dates: the first emergence of the [*O* III] emissions, the time when $H\beta$ equals λ 5007, and the equality of $H\beta$ and λ 4959.

Not all novae show all these stages. As examples, Nova Herculis never had *N* III absorption, λ 4097 and λ 4103, clearly developed, and Nova Cygni never showed a distinct Orion spectrum. In some cases it has been necessary to exercise considerable judgment as to the interpretation of apparently ambiguous phenomena. Thus, Nova Geminorum seems to have been unique in showing two absorption systems (Stratton's II and III) which might be called diffuse enhanced spectra. The writer has chosen absorption II as the principal spectrum and III as the diffuse enhanced spectrum, since they behaved in a manner similar to those systems in other novae. The set of fine lines called absorption I by Stratton lasted too briefly after maximum light to warrant calling it the principal spectrum. Nova Pictoris offered some difficulty in connection with the diffuse enhanced spectrum. Absorptions IV, IV*a*, and VI all answered approximately to the description of such a system. The writer has chosen VI because of its much greater strength, its greater number of lines, and its much longer persistence. If either of the others had been chosen, VI would have been an outstanding anomaly without parallel in other novae.

The expression of rates of development as a function of velocity meets with a difficulty in the variable velocity of most absorption systems. For uniformity, the velocity adopted in each case was the value at the time when the absorption system first became well developed.

In Table 1 the time intervals, measured in days from light-maximum, are given for each stage of the seven novae. The columns are arranged in order of the rate of development: Nova Lacertae is first and Nova Pictoris is last. At the head of each column the velocity of the principal absorption spectrum is given. There is room here

for differences of interpretation, as pointed out above in the case of Nova Geminorum. Nova Lacertae[6] and Nova Aquilae[7] had principal spectra so close to the positions of their premaximum spectra that it would be easy to mistake them for one absorption system of varying displacement.

The estimation of dates of appearance or disappearance of absorption spectra involves the use of considerable judgment. Feeble

TABLE 1

DATES OF SPECTROSCOPIC STAGES

	Nova Lac 1936	Nova Aql 1918	Nova Per 1901	Nova Gem 1912	Nova Cyg 1920	Nova Her 1934	Nova Pic 1925
Velocity of the principal spectrum (km/sec)	1500	1500	1300	800	700	315	285
Change B to A	− 1d0	*	− 1d0	.....	†	− 8d5	‡
Maximum light	0.0	0d0	0.0	0d0	0d0	0.0	0d0
Appearance of principal spectrum	+ 0.5:	+ 0.5:	+ 0.5:	+ 2.5	+ 0.8	+ 3.	+ 1.0
Appearance of diffuse enhanced spectrum	1.5	0.5:	.....	4.5	3.2	13.	47.
Maximum of diffuse enhanced spectrum	3.7	2.6	.....	10.4	9.	39.	78.
Disappearance of diffuse enhanced spectrum	5.7	6.1	.....	14.4	15.	87.	157.
Appearance of Orion spectrum	2.5	4.1	.....	9.4	.....	71.	148.
Maximum of Orion spectrum	4.7	7.	.....	20.	.....	96.	178.
Disappearance of Orion spectrum	10.	11.	.....	.....	.....	103.	213.
Multiple hydrogen	4.7	5.	.....	20.	21.	94.	84.
Appearance of *N* III absorption	10.	5:	.....	14.4	16.	.....	.....
Disappearance of *N* III absorption	22.	50.	.....	>270.	> 38.	.....	.....
Appearance of [*O* III] emission	22.	12.	33:	41.	> 41.	123.	253.
λ 5007 = *Hβ*	56.	83.	.....	<270.	.....	<147.	.....
λ 4959 = *Hβ*	102.	158.	.....	300.	.....	210.	.....

* The change of spectrum between June 8 and 9, from class Ao to about A5, indicates a possible B type more than 1.3 days before maximum.

† A change from Ao to about A2 was recorded between August 22.7 and 23.6. A possible change from B to A would have to be at least 1.5 days before maximum.

‡ During 14 days before maximum the spectrum was class F5. However, the nova was bright 56 days before maximum, and there was ample time for spectral changes.

traces were not considered sufficient for the purpose of this investigation. A spectrum was considered to be just appearing or disappearing when its lines were quite distinct without being conspicuous. Some attempt was made to allow for the character of the lines. Thus, although the diffuse enhanced spectrum in Nova Herculis is recorded as disappearing March 19, very narrow components remained until March 29. Had they been more diffuse, they would not have been seen after March 20. Since the study is a comparative one, the most

[6] McLaughlin, *Pub. A.A.S.*, **8**, 248, 1936.

[7] McLaughlin, *Ap. J.*, **84**, 106, 1936.

important consideration is that the criteria should be uniform for all the novae. To that end the writer based his final judgment upon examination of the Ann Arbor plates and of the reproductions of the spectrum of Nova Pictoris.

In Table 2 the differences between the visual magnitude at each stage and the magnitude at maximum are tabulated in the same order as in Table 1. Opposite the entry "Maximum light" in the

TABLE 2

MAGNITUDE DROP FROM MAXIMUM AT EACH PHASE

	Nova Lac 1936	Nova Aql 1918	Nova Per 1901	Nova Gem 1912	Nova Cyg 1920	Nova Her 1934	Nova Pic 1925
Change B to A	0^M6	$>2^M$*	0^M6	.....	$>1^M$*	1^M8	.....
Maximum light	[2.1]	[−1.1]	[0.2]	[3^M6]	[2.0]	[1.4]	[1^M2]
Appearance of principal spectrum	0.4	1:	0.2	1.2:	0.1	(1.0)	0.1
Appearance of diffuse enhanced spectrum	0.9	1:	.....	(1.4)	1.0	(1.2)	(1.3)
Maximum of diffuse enhanced spectrum	1.7	1.9	.....	(1.8)	1.3	(1.6)	(2.1)
Disappearance of diffuse enhanced spectrum	2.3	2.9	.....	(2.0)	2.9	(2.7)	3.1
Appearance of Orion spectrum	1.3	2.3	.....	(1.8)	.....	2.2	2.9
Maximum of Orion spectrum	2.1	3.1	.....	2.2	.....	3.2	3.1
Disappearance of Orion spectrum	3.1	3.6	.....	.....	.....	3.4	3.4
Multiple hydrogen	2.3	2.6	.....	2.2	3.5	(2.9)	2.2
Appearance of *N* III absorption	3.1	2.6:	.....	2.4	2.9	.....	.....
Disappearance of *N* III absorption	4.1	5.1	.....	.....	5.2	.....	.....
Appearance of [*O* III] emission	4.1	3.7	4.2:	3.2	5.6	(3.4)	(3.8)
λ 5007 = $H\beta$	5.1	6.0	.....	4.3	.....	(3.8)	.....
λ 4959 = $H\beta$	5.6	6.6	.....	4.8	.....	(5.1)	.....

* Conjectural.

first column the visual magnitude of maximum is given in square brackets. The data were taken from light-curves from which the secondary fluctuations had been smoothed out. The sources were Jones's light-curve of Nova Pictoris, the writer's curves of Nova Herculis and Nova Lacertae, and the Harvard light-curves[8] for the remaining stars. In the case of Nova Herculis the curve was drawn straight across the great minimum of May, 1935, at a uniform rate of decline. All values taken from smoothed portions of the curves are inclosed in parentheses in Table 2.

[8] Nova Persei, *Harvard Ann.*, **48**, 39, 1903; Nova Geminorum, *ibid.*, **76**, 191, 1915; Nova Aquilae, *ibid.*, **81**, 113, 1919; Nova Cygni, *Harvard Bull.*, No. 890, 1932.

Inspection of Table 1 shows a general increase of the time of development from left to right, with the decrease of absorption velocity. In Table 2, however, there is no evident systematic difference from column to column. Thus, while a slow nova shows slower development of its spectrum, its light also declines more slowly, with the result that the difference in magnitude between maximum and each spectroscopic phase is unrelated to the rate of development.

TABLE 3

AVERAGE MAGNITUDES AND REDUCED TIMES FOR STAGES OF A TYPICAL NOVA

Stage	Magnitude Difference	Time from Maximum Light
Change B to A	$1^{M}0$	$-\ 1^{d}5$
Maximum light	0.0	0.0
Appearance of principal spectrum	0.5	+ 0.6
Appearance of diffuse enhanced spectrum	1.1	2.0
Maximum of diffuse enhanced spectrum	1.7	3.6
Appearance of Orion spectrum	2.2	5.2
Multiple hydrogen	2.5	6.3
Maximum of Orion spectrum	2.7	7.2
Disappearance of diffuse enhanced spectrum	2.7	7.2
Appearance of *N* III absorption	2.7	7.2
Disappearance of Orion spectrum	3.4	13.
Appearance of [*O* III] emission	3.7	17.
Disappearance of *N* III absorption	5.0:	54:
λ 5007 = $H\beta$	5.1	56.
λ 4959 = $H\beta$	5.7	110:

In order to compare the novae the differences in magnitude in Table 2 were averaged for each stage, giving the values in the second column of Table 3, where they are arranged in numerical order. Some less reliable values were assigned low weight. Corresponding to the average magnitude drop, the time interval in days from maximum was read from the light-curve of Nova Lacertae—the smoothest of all the curves, and the one of most rapid decline. These intervals are given in the third column of Table 3, which is essentially a chronology of an average nova, reduced to the time scale of the most rapid of the bright novae.

For each nova the time intervals for each stage in Table 1 were plotted as ordinates against the corresponding values in Table 3 as abscissae. For all stages previous to the disappearance of the Orion absorptions, the points for each nova were found to lie reasonably close to a straight line. In the later stages Nova Herculis and Nova Pictoris appeared to develop more rapidly than the linear relation indicated. The plots are shown in Figure 1.

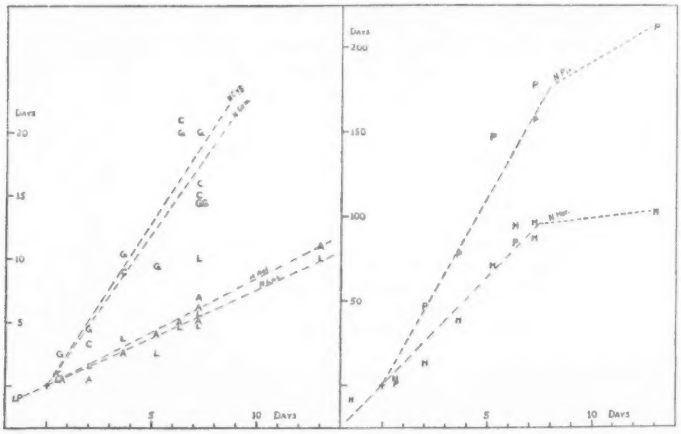

FIG. 1.—Comparison of times of spectroscopic stages of six novae. The abscissae are the average reduced times from maximum light (third column of Table 3). The ordinates are the observed time intervals from maximum (Table 1). The left half of the diagram shows Nova Geminorum 1912 (*G*), Nova Aquilae 1918 (*A*), Nova Cygni 1920 (*C*), and Nova Lacertae 1936 (*L*). The point for the B–A transition of Nova Persei 1901 (*P*) is also shown. The right half shows Nova Pictoris 1925 (*P*) and Nova Herculis 1934 (*H*).

Slopes measured on the plots give the relative times of development tabulated in the second column of Table 4, where the time for Nova Lacertae (not the average) is taken as the unit. The third and fourth columns contain the velocities of the principal and diffuse enhanced spectra, respectively, at the times of their first conspicuous development. The values in the last two columns were computed from formulae derived below. The time of development given for Nova Persei depends mainly upon the light-curve, since the spectroscopic phases are not well determined.

The times and velocities for the six well-observed novae fall into

three pairs. Plots of log V_1 and log V_2 against log t indicated linear relations, and the following formulae were derived by the method of least squares:

$$\log_{10} V_1 = 3.19 - 0.54 \log_{10} t ,$$

$$\log_{10} V_2 = 3.39 - 0.39 \log_{10} t .$$

The velocities given in the last two columns of Table 4 were computed by means of these formulae. The agreement of the observed and the computed velocities is very satisfactory.

TABLE 4

Nova	Time (Nova Lac = 1)	Velocities in Km/Sec			
		Observed		Computed	
		V_1	V_2	V_1	V_2
Lacertae	1.0	1500	3000	1550	2450
Aquilae	1.1	1500	2200	1470	2360
Persei	(1.8)	1300	?	1130	1950
Geminorum	3.1	800	1500	840	1575
Cygni	3.4	700	1400	795	1520
Herculis	16.	315	800	346	830
Pictoris	28.	285	750:*	257	668

* The diffuse enhanced spectrum of Nova Pictoris was composite. The value chosen is a rough mean velocity of the several components.

If we define the rate of development, r, by the relation $r = 1/t$, we then have, approximately:

$$r \sim V_1^2 \qquad \text{and} \qquad r \sim V_2^{5/2} .$$

Data for the nebular stage are not so accordant. Thus, although Nova Herculis took considerably longer to develop to the Orion stage than did Nova Geminorum, it reached equality of $H\beta$ and λ 4959 in a shorter time. If we use only the intervals in days from maximum light to the first appearance of the [*O* III] emissions (designated t_n), the following relation is obtained:

$$\log_{10} V_1 = 4.0 - 0.65 \log_{10} t_n .$$

Defining the rate as before, we then have, approximately:

$$r_n \sim V_1^{3/2}.$$

In the present condition of the problem it would be unwise to base a physical model on the empirical relations derived above. It has been pointed out that judgment played a certain part in the selection of the velocities used. With only six well-determined rates it would be an unwarranted generalization to regard the formulae as expressions of some law of nova activity. On the other hand, the representation of the data by the formulae is so good that it does not appear reasonable to dismiss the relations as fortuitous.

If the state of a nova spectrum depended only on the density of the ejected gases, and if the thickness of the shell remained the same fraction of the radius at all times during the expansion, we should have for the rate of development $r \sim V^3$. If the thickness of the shell remained constant, we should have $r \sim V^2$. The same relation would be obtained if the development were independent of the density and depended only on the intensity of radiation received from an invariable stellar nucleus. Although all these conditions are too simplified to represent even approximately the conditions of a nova outburst, the exponent of V determined by three methods of approach is of the expected order of magnitude.

It is a little surprising that the several stages in different novae follow such an orderly sequence. The initial outburst would be expected to determine the behavior of the principal spectrum, but it is not evident a priori that it should indicate the rate of development of other absorption systems, which presumably originate in different parts of the ejected material. Likewise, if the continuous spectrum originated in a central nucleus, we should hardly expect the fading of the light to follow such a uniform course with respect to the spectral changes; in particular, we should expect it to be independent of the velocity. On the other hand, if the continuous spectrum originated in an ejected shell or shells, in radiative equilibrium with a central nucleus, a relation between the velocity and the rate of decline of light would be expected.

Speculating a little more freely, the fact that we can express the

rate of development in terms of a single parameter—the velocity—suggests that the phenomenon of a nova is due to a single sudden[9] release of energy within the star. The great explosion represented by the rise to maximum light determines completely the train of events which follows during months or years afterward, just as the trajectories of the fragments of a bursting bomb are determined at the instant of the explosion. Whatever differences we observe between the spectra of novae having equal rates of development would then depend upon chance irregularities in the density of the ejected matter, on the composition and degree of turbulence of the gases, and on the orientation of the main erupted masses with respect to the line of sight.

The slow and rapid novae appear to differ only as the adjectives indicate; their phenomena are essentially similar. Because only seven bright novae have been intensively observed, our statistical data are woefully incomplete. It appears possible that future novae will help to fill the apparent gaps between the three pairs now recognized and that the apparent demarcation between slow and rapid novae will eventually disappear.

THE OBSERVATORY
UNIVERSITY OF MICHIGAN
March 27, 1937

[9] "Sudden," as used here, is not to be taken as implying an instantaneous release. The process of release might occupy an interval of several days, but it is thought of as continuous—not as a series of separate outbursts.

THE PRESSURE IN THE INTERIOR OF A STAR

S. CHANDRASEKHAR

ABSTRACT

In this paper certain integral theorems on the equilibrium of a star are proved.

I

In a recent paper[1] the author proved the following theorems:

THEOREM 1.—*In any equilibrium configuration in which the mean density inside* r *decreases outward, we have the inequality*

$$\tfrac{1}{2}G(\tfrac{4}{3}\pi)^{1/3}\bar{\rho}^{4/3}(r)M^{2/3}(r) \leqslant P_c - P \leqslant \tfrac{1}{2}G(\tfrac{4}{3}\pi)^{1/3}\rho_c^{4/3}M^{2/3}(r)\,, \quad (1)$$

where $\bar{\rho}$ (r) *denotes the mean density inside* r, ρ_c *the central density,* P_c *the central pressure, and* M(r) *the mass inclosed inside* r.

THEOREM 2.—*If* $(1 - \beta_c)$ *is the ratio of the radiation pressure to the total pressure at the center of a wholly gaseous configuration, then under the conditions of Theorem 1*

$$1 - \beta_c \leqslant 1 - \beta^*\,, \quad (2)$$

where $(1-\beta^*)$ *satisfies the quartic equation*

$$M = \left(\frac{6}{\pi}\right)^{1/2}\left[\left(\frac{k}{\mu H}\right)^4 \frac{3}{a}\frac{1-\beta^*}{\beta^{*4}}\right]^{1/2}\frac{1}{G^{3/2}}\,. \quad (3)$$

THEOREM 3.—*If* I_ν *is the integral defined by*

$$I_\nu = \int_0^R \frac{GM(r)dM(r)}{r^\nu}\,, \qquad (\nu < 6)\,, \quad (4)$$

where R *denotes the radius of the configuration, then*

$$\frac{3}{6-\nu}\,G(\tfrac{4}{3}\pi\bar{\rho})^{\nu/3}M^{(6-\nu)/3} \leqslant I_\nu \leqslant \frac{3}{6-\nu}\,G(\tfrac{4}{3}\pi\rho_c)^{\nu/3}M^{(6-\nu)/3}\,. \quad (5)$$

[1] *M.N.*, **96**, 644, 1936. See also E. A. Milne, *ibid.*, 179.

II

In this paper we shall prove certain additional theorems on the equilibrium of a star.

THEOREM 4.—*Under the conditions of Theorem 1 we have*

$$\frac{P_c}{\rho_c^{\nu/3}} \leqslant \frac{1}{6-\nu}\left(\tfrac{4}{3}\pi\right)^{(\nu-3)/3} G R^{\nu-4} M^{(6-\nu)/3}, \tag{6}$$

provided

$$6 > \nu \geqslant 4, \tag{7}$$

where (6) *is a strict inequality for* $\nu > 4$.

Proof: We have equation 7 (*loc. cit.*)

$$dP = -\frac{G}{4\pi}\frac{M(r)dM(r)}{r^4}. \tag{8}$$

Introducing equation (8) in equation (4), we have

$$I_\nu = -4\pi\int_0^R \frac{dP}{r^{\nu-4}}. \tag{9}$$

Since $\nu \geqslant 4$, we clearly have

$$I_\nu \geqslant -\frac{4\pi}{R^{\nu-4}}\int_0^R dP = \frac{4\pi}{R^{\nu-4}} P_c. \tag{10}$$

In equation (10) we have the equality sign only for the case $\nu = 4$. For $\nu > 4$ we have a strict inequality.

Combining equation (10) with the inequality of Theorem 3, we have

$$\frac{4\pi}{R^{\nu-4}} P_c \leqslant I_\nu \leqslant \frac{3}{6-\nu} G\left(\tfrac{4}{3}\pi\rho_c\right)^{\nu/3} M^{(6-\nu)/3} \tag{11}$$

or

$$\frac{P_c}{\rho_c^{\nu/3}} \leqslant \frac{1}{6-\nu}\left(\tfrac{4}{3}\pi\right)^{(\nu-3)/3} G R^{\nu-4} M^{(6-\nu)/3}. \tag{12}$$

Again, equation (12) is a strict inequality for $\nu > 4$. This proves the theorem.

III

Comments on Theorem 4.—When $\nu = 4$, equation (12) reduces to an inequality from which Theorem 2 would immediately follow. If we write

$$\nu = 3\left(1 + \frac{1}{n}\right), \tag{13}$$

then we can re-write equation (12) as

$$\frac{P_c}{\rho_c^{(n+1)/n}} \leqslant S_n G\, R^{(3-n)/n} M^{(n-1)/n}, \qquad (1 < n \leqslant 3), \tag{14}$$

where S_n stands for the numerical coefficient

$$S_n = (\tfrac{4}{3}\pi)^{1/n} \frac{n}{3(n-1)}. \tag{15}$$

Equations (14) and (15) bring out the very general "critical" nature of $n = 1$ and $n = 3$, a circumstance only very partially disclosed in the theory of polytropes. For, if we consider a polytrope of index n, then of course

$$\frac{P}{\rho^{(n+1)/n}} = \text{Constant} = \frac{P_c}{\rho_c^{(n+1)/n}}. \tag{16}$$

For the polytropic case (16) we have

$$\frac{P_c}{\rho_c^{(n+1)/n}} = T_n G\, R^{(3-n)/n} M^{(n-1)/n}, \tag{17}$$

where

$$T_n = \frac{1}{(n+1)} \left(\frac{4\pi}{\omega_n^{n-1}}\right)^{1/n}, \tag{18}$$

$$\omega_n = -\left(\xi^{\frac{n+1}{n-1}} \frac{d\theta_n}{d\xi}\right)_{\xi=\xi_1}. \tag{19}$$

The symbols ξ and θ stand for the Emden variables, θ_n is *any* Emden solution of index n, and the quantity in brackets in equation (19) has to be taken at the first zero $\xi = \xi_1$ of the Emden solution.[2]

[2] An Emden solution of index n is a function which satisfies Emden's equation of index n and is finite at the origin. Equation (19) can be evaluated at the boundary of any Emden solution because it is homology invariant.

Table I gives the values of S_n and T_n for different values of n.

TABLE I

n	S_n	T_n	S_n/T_n
3.0	0.806	0.364	2.214
2.5	0.985	.351	2.803
2.0	1.364	.365	3.741
1.5	2.599	.424	6.125
1.0	∞	0.637	∞

IV

THEOREM 5.—*If* $I_{\sigma,\nu}$ *stands for the integral*

$$I_{\sigma,\nu} = \int_0^R \frac{GM^\sigma(r)dM(r)}{r^\nu}, \qquad [3(\sigma+1) > \nu], \tag{20}$$

then under the conditions of Theorem 1

$$\frac{3}{3\sigma+3-\nu}\frac{GM^{\sigma+1}}{\xi^\nu} \geqslant I_{\sigma,\nu} \geqslant \frac{3}{3\sigma+3-\nu}\frac{GM^{\sigma+1}}{R^\nu}, \tag{21}$$

where ξ *is defined by the relation*

$$\tfrac{4}{3}\pi\rho_c\xi^3 = M. \tag{22}$$

Proof: Since

$$r^\nu = \left[\frac{M(r)}{\tfrac{4}{3}\pi\bar{\rho}(r)}\right]^{\nu/3}, \tag{23}$$

we have from equation (20) that

$$I_{\sigma,\nu} = G(\tfrac{4}{3}\pi)^{\nu/3}\int_0^R \rho^{\nu/3}(r)M^{(3\sigma-\nu)/3}dM(r). \tag{24}$$

Since we have assumed that $\bar{\rho}(r)$ decreases outward, it is clear that the minimum value of equation (24) is obtained by replacing $\bar{\rho}(r)$ by its minimum $\bar{\rho}$ (the mean density for the whole configuration) and taking it out of the integral sign. In the same way the maximum

value of equation (24) is obtained by replacing $\bar{\rho}(r)$ by its maximum value ρ_c and taking it out of the integral sign. One thus finds that

$$\left.\begin{aligned} \frac{3}{3\sigma+3-\nu} G(\tfrac{4}{3}\pi\bar{\rho})^{\nu/3} M^{(3\sigma+3-\nu)/3} &\leqslant I_{\sigma,\nu} \\ &\leqslant \frac{3}{3\sigma+3-\nu} G(\tfrac{4}{3}\pi\rho_c)^{\nu/3} \cdot M^{(3\sigma+3-\nu)/3}, \end{aligned}\right\} \tag{25}$$

which is easily seen to be equivalent to equation (21).

V

THEOREM 6.—*If* $\bar{P}_{p,q}$ *is the mean pressure defined by*

$$M^p R^q \bar{P}_{p,q} = \int_0^R P d(M^p(r) r^q), \qquad (p, q > 0), \tag{26}$$

then under the conditions of Theorem 1

$$\bar{P}_{p,q} \geqslant \frac{3}{4\pi} \frac{1}{3p+q+2} \frac{GM^2}{R^4}. \tag{27}$$

Proof: Integrating equation (26) by parts, we have

$$M^p R^q \bar{P}_{p,q} = -\int_0^R M^p(r) r^q dP. \tag{28}$$

By equation (8) we have

$$M^p R^q \bar{P}_{p,q} = \frac{1}{4\pi} \int_0^R \frac{GM^{p+1}(r) dM(r)}{r^{4-q}}, \tag{29}$$

$$= \frac{1}{4\pi} I_{p+1,4-q}. \tag{30}$$

Hence, by Theorem 5 we easily find that

$$\bar{P}_{p,q} \geqslant \frac{3}{4\pi} \frac{1}{3p+q+2} \frac{GM^2}{R^4}, \tag{31}$$

which proves the theorem.

VI

THEOREM 7.—*In a wholly gaseous configuration in which the mean density inside* r, *the temperature, and the ratio of the radiation pressure to the total pressure decrease outward, we have*

$$T_c > \tfrac{1}{6}\frac{\mu H}{k}\frac{GM}{R}\beta^* , \tag{32}$$

where T_c *is the central temperature,* β^* *has the same meaning as in Theorem 2 and* μ, H, *and* k *are, respectively, the mean molecular weight (assumed constant in the whole configuration), the mass of the proton, and the Boltzmann constant.*

Proof: Let $\bar{P}$ denote the mean pressure defined by

$$R^3\bar{P} = \int_0^R P d(r^3) . \tag{33}$$

By equation (31)

$$\bar{P} \geqslant \frac{3}{20\pi}\frac{GM^2}{R^4} = \tfrac{1}{6}(\tfrac{4}{3}\pi)^{1/3}G\bar{\rho}^{4/3}M^{2/3} . \tag{34}$$

In a wholly gaseous configuration

$$P = \frac{k}{\mu H}\beta^{-1}\rho T . \tag{35}$$

Hence

$$\bar{P} = \frac{k}{\mu H}\overline{(\beta^{-1}\rho T)} . \tag{36}$$

Since $(1 - \beta)$ is assumed to decrease outward, β must increase outward, and hence

$$\bar{P} < \frac{k}{\mu H}\beta_c^{-1}T_c\bar{\rho} , \tag{37}$$

where $\bar{\rho}$ is now the mean density defined in the usual way, since the means we are now taking are weighted according to the volume element; compare equation (33). Hence

$$T_c > \tfrac{1}{6}\frac{\mu H}{k}G(\tfrac{4}{3}\pi\bar{\rho})^{1/3}M^{2/3}\beta_c , \tag{38}$$

or

$$T_c > \tfrac{1}{5}\frac{\mu H}{k}\frac{GM}{R}\beta_c\,. \tag{39}$$

But by Theorem 2

$$\beta_c \geqslant \beta^*\,, \tag{40}$$

where β^* satisfies the quartic equation (3). Hence, combining equations (39) and (40), we have

$$T_c > \tfrac{1}{5}\frac{\mu H}{k}\frac{GM}{R}\beta^*\,, \tag{41}$$

which proves the theorem.

The inequality equation (41) is not a "best possible" one, but it has the advantage of not neglecting the radiation pressure and is, in fact, the first of the kind to be established.

We notice that the *mean* temperature $\overline{T}$, defined by

$$M\overline{T} = \int_0^R T dM(r)\,,$$

satisfies the same inequality as T_c. For

$$M\overline{T} = \int_0^R T dM(r) = \frac{\mu H}{k}\int_0^R \beta P\rho^{-1} dM(r)\,.$$

$$= \frac{\mu H}{k}\int_0^R \beta P dv\,,$$

where dv is the volume element. But since β is assumed to increase outward,

$$M\overline{T} \geqslant \frac{\mu H}{k}\beta_c\int_0^R P dv = \tfrac{1}{3}\frac{\mu H}{k}\beta_c\Omega\,,$$

where Ω is the negative potential energy of the configuration. But by Theorem 3,

$$\Omega = I_1 \geqslant \tfrac{3}{5}\frac{GM^2}{R}\,.$$

Hence

$$\bar{T} \geqslant \tfrac{1}{5}\frac{\mu H}{k}\frac{GM}{R}\beta_c \geqslant \tfrac{1}{5}\frac{\mu H}{k}\frac{GM}{R}\beta^* .$$

VII

Corollary to Theorem 7.—In a wholly gaseous configuration in which the mean density inside r *and the ratio of the radiation pressure to the total pressure decreases outward, we have*

$$M < \left(2.5\,\frac{\overline{(\rho^{4/3})}}{(\bar{\rho})^{4/3}}\right)^{3/2}\left(\frac{6}{\pi}\right)^{1/2}\left[\left(\frac{k}{\mu H}\right)^4\frac{3}{a}\frac{1-\beta_c}{\beta_c^4}\right]^{1/2}\frac{1}{G^{3/2}}. \tag{42}$$

Proof: Equation (35) can also be written

$$P = \left[\left(\frac{k}{\mu H}\right)^4\frac{3}{a}\frac{1-\beta}{\beta^4}\right]^{1/3}\rho^{4/3}, \tag{43}$$

so that

$$\bar{P} = \overline{\left[\left(\frac{k}{\mu H}\right)^4\frac{3}{a}\frac{1-\beta}{\beta^4}\right]^{1/3}\rho^{4/3}}, \tag{44}$$

or, since $(1-\beta)$ decreases outward,

$$\bar{P} < \left[\left(\frac{k}{\mu H}\right)^4\frac{3}{a}\frac{1-\beta_c}{\beta_c^4}\right]^{1/3}\overline{(\rho^{4/3})} . \tag{45}$$

Combining equations (45) and (34), we have

$$\left[\left(\frac{k}{\mu H}\right)^4\frac{3}{a}\frac{1-\beta_c}{\beta_c^4}\right]^{1/3}\overline{(\rho^{4/3})} > \tfrac{1}{5}(\tfrac{4}{3}\pi)^{1/3}G\bar{\rho}^{4/3}M^{2/3}, \tag{46}$$

which, after some minor transformation, goes over into equation (42).

It may be noticed that in equation (42) we cannot replace $\overline{(\rho^{4/3})}/(\bar{\rho})^{4/3}$ by unity, since

$$\overline{(\rho^{4/3})} > (\bar{\rho})^{4/3} . \tag{47}$$

Equation (42) is not a "best possible" inequality, but it is much "sharper" than the inequality established previously.[3]

YERKES OBSERVATORY
April 12, 1937

[3] Equation (19′) (*loc. cit.*).

ON THE SPECTRAL CLASSIFICATION OF THE STARS OF TYPES A TO K

W. W. MORGAN

ABSTRACT

An interpretation of the absolute-magnitude–spectral-type diagram is made in terms of the physical parameters effective temperature and surface gravity. Stars belonging to the main sequence are shown to have the characteristic of approximately constant surface gravity, and the fundamental nature of the effective-temperature–surface-gravity diagram is pointed out.

The advantages of a two-dimensional empirical spectral classification are discussed. A practical two-dimensional classification system is outlined which can be employed with small-scale spectrograms. The determination of absolute magnitude by the line-ratio method is shown to be feasible for stars of types F5 to K9, from spectrograms of considerably lower dispersion than has been used previously.[1]

I

1. The two fundamental physical factors which define the surface conditions of a star are the effective temperature, which is a measure of the rate of outflow of radiant heat per unit area, and the surface gravity. The principal spectral changes noted on passing along the Draper Sequence are due to changes in the effective temperature; lines whose intensities change considerably with luminosity are sensitive to variations in surface gravity.

The Draper classification is not, however, a pure temperature classification; in order to define the effective temperature of a star uniquely, it is necessary to specify both the spectral type and the absolute magnitude. This is necessary because of the considerable variation of temperature with luminosity within a single spectral subdivision. For this reason the Russell diagram, which gives absolute magnitude as a function of spectral type, does not separate the physical variables completely.

If the validity of the Planck formula and the mass-luminosity relationship are assumed, it is possible to determine the parameters Te and g from a combination of color index and absolute magnitude.[2] If

[1] I am indebted to Miss Dorritt Hoffleit for pointing out that low-dispersion objective-prism plates were used earlier by Shapley (*Harvard Bull.*, **788**).

[2] As Eddington has pointed out (*Internal Constitution of the Stars*, p. 140), the color temperature is not strictly identical with the effective temperature; in view of the prac-

the color index, I, is expressed on King's scale, the color temperature is

$$T = \frac{7200}{I + 0.64}. \tag{1}$$

The stellar radius is determined from

$$\log R = 0.82I - 0.20M_v + 0.51, \tag{2}$$

where M_v is the visual absolute magnitude. These formulae are derived from Planck's formula in Volume II of *Astronomy* by Russell, Dugan, and Stewart. If the mass is determined from the mass-luminosity relationship, the value of g, the surface gravity, is determined in units, $\odot = 1$, from

$$g = \frac{M}{R^2}. \tag{3}$$

The justification of the application of the Planck formula to stellar radiation may be questioned because of recent work which has shown that stellar energy-curves deviate from those expected from black-body radiation. When color indices on King's scale are used, the resulting temperatures are in fair agreement with those determined in other ways; and we may consider equation (1) as an empirical formula which gives a somewhat idealized temperature scale which is in good agreement with other determinations. The same remarks also apply to equation (2), which can be modified to give the stellar diameter in seconds of arc when the absolute magnitude is unknown:

$$\log d'' = 0.82I - 0.20m_v - 2.52, \tag{4}$$

where m_v is the visual apparent magnitude of the star. A comparison of diameters computed from equation (4) with those determined with the interferometer at Mount Wilson shows that the results are in good agreement.[3] The eclipsing systems β Aurigae and Castor C,

---

tical uncertainties involved, however, the former can be used as an approximation to the latter.

[3] See Russell, Dugan, and Stewart, *Astronomy*, Vol. 2.

which are located at the extremities of the spectral range discussed here and have fairly well-determined trigonometric parallaxes, also show good agreement between the diameters obtained from the color indices and those determined from the eclipsing and spectroscopic elements and the parallax. The results for these two systems are summarized in Table 1.

The orbital radii are those from the photometric solutions based on the assumption of uniformly illuminated stellar disks. The sources of the other data are listed in connection with Table 3. From a comparison with interferometric diameters of the red giants and

TABLE 1

APPARENT DIAMETERS OF ECLIPSING BINARIES

Star	Spectrum	Trig π	log d'' (Orbit)	I	log d'' (I)
β Aurigae $\frac{A+B}{2}$	A0	0.037±4	3.01	0.08	3.05
YY Geminorum $\frac{A+B}{2}$	dM1	0.073±3	3.31	1.38	3.38

orbital values of the main sequence binaries β Aurigae and YY Geminorum, the use of formula (2) is shown to give accordant results for color indices expressed on King's scale.

2. A representative sequence of stars was selected in the following groups: (*a*) Nine supergiants. These are all well-known c-stars. For the cA stars α Cygni and σ Cygni, the visual absolute magnitudes were considered to be − 5.5 mag. from a comparison with the absolute magnitudes of stars having similar spectra in the double cluster in Perseus. An approximate upper limit on the luminosity of the white c-stars is set by the brightest objects observed in near-by extragalactic objects, which average about −6 mag., according to Hubble.[4] An approximate lower limit can be determined from the extremely small proper motions and trigonometric parallaxes of the cA stars. For the cF7 star α Ursae Minoris, the absolute magnitude of −3.9 was determined by comparison with its ninth-magni-

[4] *Ap. J.* **84**, 285, 1936.

tude physical companion, which is, according to Mount Wilson, an early F-type main-sequence star. The F7 supergiant γ Cygni gives spectroscopic evidence of being more luminous than α Ursae Minoris, and its absolute magnitude has been rather arbitrarily set at -4.5. The absolute magnitudes of the other c-stars have been taken from the determinations by Öpik,[5] which are based on a combination of proper motions, colors, and spectral types. In spite of the rather uncertain approximations which are necessary in order to determine the luminosities of the c-stars, it is thought that the absolute magnitudes are not in error by more than about 1.5 mag. at the greatest. (*b*) Six bright "normal" giants. These are bright stars with fairly well-determined trigonometric parallaxes. The parallax of α Aurigae is that determined from the orbit and the interferometer measures. A Yerkes three-prism spectrogram of α Aurigae fails to show any appreciable difference in the relative intensities of the stronger Ti^{+} lines due to the two components in the $\lambda\lambda$ 4500–4600 region, and their apparent magnitudes have been considered equal. (*c*) Three bright "subgiants" having well-determined trigonometric parallaxes. (*d*) Thirty-eight main-sequence stars having large, well-determined trigonometric parallaxes. (*e*) The white dwarf o^2 Eridani B.

All of the stars selected under (*a*), (*b*), (*c*), and (*d*) are included in Öpik's catalogue of carefully discussed color indices.[5] These color indices are of a high order of accuracy and are well suited to the determination of the color temperatures and radii. They are not on the color scale of King, but Öpik gives data by which they may be transformed to the scale for which formulae (1) and (2) have been found to be valid. The color-temperature scale defined by formula (1) and by Öpik's reduced color indices is given in Table 2.

The data for the standard stars are given in Table 3. The columns give for each star: (1) the serial number in Schlesinger's stellar parallax catalogue for 1935; (2) the name; (3) the spectral type (the Victoria type has been used for all stars for which it has been determined; the Mount Wilson type has been used for other stars later than F4; the Henry Draper types are used for stars not included in the Victoria catalogue whose spectral types are earlier than F5); (4) the HR visual magnitude; (5) the trigonometric parallax for all

[5] *Tartu Pub.*, **27**, Part I, 1929.

stars except the supergiants; (6) the visual absolute magnitude; (7) the color index from Öpik's catalogue reduced to King's scale; (8) the bolometric absolute magnitude determined according to Eddington's definition; (9) the logarithm of the mass as determined from Eddington's mass-luminosity relationship; (10) the logarithm of the radius determined from the color and from the absolute magnitude; (11) the value of log g determined from the mass and the radius (the sun's mass, radius, and surface gravity are taken as units); (12) the logarithm of the color temperature.

TABLE 2

COLOR-TEMPERATURE SCALE DEFINED BY ÖPIK'S REDUCED COLOR INDICES AND THE FORMULA $T = \frac{7200}{I + 0.64}$

Main Sequence			Supergiants		
Spectrum	I	T	Spectrum	I	T
A0	0.06	10,300	A0	0.07	10,200
A5	0.26	8,000	A2	0.10	9,800
F0	0.35	7,300	F2	0.44	6,700
F5	0.43	6,700	F7	0.58	5,900
G0	0.59	5,900	G0	1.15	4,000
G5	0.70	5,400	G9	1.47	3,400
K0	0.86	4,800	K2	1.59	3,200
K5	1.10	4,100	M1	1.77	3,000
Ma	1.42	3,500	.....	.....	.....

The Russell diagram for the stars in Table 3 is shown in Figure 1; in Figure 2 the values of log g and log T are used as arguments. The steep slope of the main sequence in the Russell diagram disappears, and the main sequence is shown to have the characteristic of approximately constant surface gravity over the whole range from A0 to M. There is a slight slope remaining which is probably real, as it is also shown for the values of g determined by an independent method for the eclipsing binaries β Aurigae and Castor C. Each successive luminosity group is separated in g from the others. The decrease in g on passing to lower temperatures is shown for the supergiants and the giants. The diagram shown in Figure 2 is of a fundamental nature, as the positions of the stars are determined explicitly as functions of the two fundamental surface parameters.

TABLE 3

Schlesinger	Star	Spec.	m_{vis}	Trig π	M_{vis}	I	M_{bol}	log Mass	log R	log g	log T_B
6612.....	σ Cyg	A0	4.28	.....	− 5.5	+0.07	− 5.8	+1.59	+1.67	−1.75	4.01
6383.....	α Cyg	A2	1.33	.....	− 5.5	+0.10	− 5.8	+1.59	+1.69	−1.79	3.99
1569.....	ϵ Aur	F2	(3.3)	.....	− 4.6	+0.44	− 4.6	+1.40	+1.79	−2.18	3.83
433.....	α UMi	F7	2.12	.....	− 3.9	+0.65	− 4.0	+1.29	+1.82	−2.35	3.75
6283.....	γ Cyg	F7	2.32	.....	− 4.5	+0.75	− 4.6	+1.44	+2.02	−2.60	3.72
7468.....	ρ Cas	G0	(4.4)	.....	− 4.5	+1.15	− 5.1	+1.61	+2.35	−3.09	3.60
2132.....	ϵ Gem	G9	3.18	.....	− 4.4	+1.47	− 5.6	+1.78	+2.59	−3.40	3.53
6756.....	ϵ Peg	K2	2.54	.....	− 4.3	+1.59	− 5.7	+1.80	+2.67	−3.54	3.51
1876.....	α Ori	M1	(0.9)	.....	− 3.3	+1.77	− 5.1	+1.69	+2.62	−3.55	3.48
1637.....	α Aur A	G1	0.96	0".063	0.0	+0.85	− 0.3	+0.63	+1.21	−1.79	3.68
2443.....	β Gem	G9	1.21	0.100±10	+ 1.2	+1.06	+ 0.7	+0.50	+1.14	−1.78	3.62
4251.....	α Boo	K0	0.24	85±4	− 0.1	+1.21	− 0.8	+0.74	+1.54	−2.34	3.59
610.....	α Ari	K2	2.23	44±5	+ 0.5	+1.20	− 0.2	+0.65	+1.41	−2.17	3.59
1424.....	α Tau	K8	1.06	46±4	− 0.6	+1.66	− 2.2	+1.03	+1.99	−2.95	3.49
346.....	β And	M0	2.37	44±6	+ 0.6	+1.62	− 0.9	+0.78	+1.72	−2.66	3.51
6417.....	η Cep	G6	3.59	69±7	+ 2.8	+0.97	+ 2.4	+0.26	+0.75	−1.24	3.65
6106.....	β Aql	G7	3.90	77±5	+ 3.3	+0.87	+ 3.0	+0.19	+0.56	−0.93	3.68
7392.....	γ Cep	K1	3.42	67±5	+ 2.6	+1.10	+ 2.0	+0.32	+0.91	−1.50	3.61
5608.....	α Lyr	A0	0.14	121±4	+ 0.6	+0.04	+ 0.2	+0.45	+0.42	−0.39	4.03
1889.....	β Aur $\frac{A+B}{2}$	A0	2.82	37±4	+ 0.7	+0.08	+ 0.4	+0.42	+0.44	−0.46	4.00
3571.....	β Leo	A2	2.23	76±5	+ 1.6	+0.20	+ 1.5	+0.31	+0.35	−0.39	3.93
6062.....	α Aql	A5	0.89	208±5	+ 2.5	+0.26	+ 2.4	+0.20	+0.22	−0.24	3.90
6627.....	α Cep	A5	2.60	77±5	+ 2.0	+0.25	+ 1.9	+0.26	+0.31	−0.36	3.91
3833.....	γ Vir $\frac{A+B}{2}$	F2	3.67	89±7	+ 3.4	+0.37	+ 3.4	+0.10	+0.13	−0.16	3.85
2423.....	α CMi	F5	0.48	291±4	+ 2.8	+0.43	+ 2.8	+0.18	+0.30	−0.42	3.83
6887.....	ι Peg	F4	3.96	77±6	+ 3.4	+0.37	+ 3.4	+0.10	+0.13	−0.16	3.85
5548.....	χ Dra	F5	3.69	119±8	+ 4.1	+0.50	+ 4.1	+0.03	+0.10	−0.17	3.80
2851.....	Boss 2413	F5	4.09	72±6	+ 3.4	+0.42	+ 3.4	+0.11	+0.17	−0.23	3.83
1508.....	ι Ori	F5	3.31	128±5	+ 3.8	+0.42	+ 3.8	+0.07	+0.09	−0.11	3.83
4744.....	γ Ser	F7	3.86	78±7	+ 3.3	+0.42	+ 3.3	+0.12	+0.19	−0.26	3.83
220.....	η Cas A	F8	3.64	182±5	+ 4.9	+0.55	+ 4.9	−0.04	−0.02	0.00	3.78
806.....	θ Per	F8	4.22	78±5	+ 3.7	+0.53	+ 3.7	+0.08	+0.20	−0.32	3.79
3576.....	β Vir	F8	3.80	101±7	+ 3.8	+0.52	+ 3.8	+0.07	+0.18	−0.29	3.79
3801.....	β CVn	G0	4.32	108±6	+ 4.5	+0.59	+ 4.5	0.00	+0.09	−0.18	3.78
1871.....	χ Ori	G1	4.62	104±6	+ 4.7	+0.58	+ 4.7	−0.02	+0.05	−0.12	3.77
3964.....	β Com	G1	4.32	134±10	+ 5.0	+0.59	+ 5.0	−0.05	+0.01	−0.07	3.78
1652.....	λ Aur	G1	4.85	68±5	+ 4.0	+0.68	+ 3.9	+0.08	+0.27	−0.46	3.73
919.....	ι Per	G1	4.17	85±4	+ 3.8	+0.62	+ 3.7	+0.09	+0.26	−0.43	3.76
660.....	δ Tri	G1	5.07	98±6	+ 5.0	+0.60	+ 5.0	−0.05	−0.02	−0.01	3.76
329.....	μ Cas	G5	5.26	130±6	+ 5.8	+0.69	+ 5.7	−0.11	0.00	−0.11	3.73
972.....	κ Cet	G5	4.96	106±5	+ 5.1	+0.64	+ 5.0	−0.05	+0.01	−0.07	3.75
3582.....	Gr 1830	G7	6.46	108±4	+ 6.6	+0.75	+ 6.5	−0.18	−0.20	+0.22	3.72
518.....	τ Cet	G7	3.65	301±7	+ 6.0	+0.77	+ 5.8	−0.12	−0.06	0.00	3.71
5996.....	σ Dra	G9	4.78	181±4	+ 6.1	+0.84	+ 5.9	−0.12	−0.02	−0.08	3.68
3015.....	11 LMi	G9	5.48	95±5	+ 5.4	+0.85	+ 5.2	−0.05	+0.13	−0.31	3.68
168.....	54 Psc	K1	6.08	104±6	+ 6.2	+0.87	+ 6.0	−0.13	−0.02	−0.09	3.68
509.....	107 Psc	K1	5.32	132±6	+ 5.9	+0.88	+ 5.6	−0.09	+0.05	−0.19	3.67
222.....	Boss 171	K4	5.82	148±6	+ 6.7	+0.87	+ 6.5	−0.17	−0.12	+0.07	3.68
7259.....	Boss 5976	K5	5.65	146±6	+ 6.5	+1.09	+ 5.9	−0.11	+0.12	−0.35	3.62
769.....	Boss 588	K7	5.92	144±5	+ 6.7	+1.00	+ 6.3	−0.15	−0.01	−0.13	3.64
6558A.....	61 Cyg A	K8	5.57	299±3	+ 8.0	+1.18	+ 7.3	−0.24	−0.12	0.00	3.59
6558B.....	61 Cyg B	K9	6.28	299±3	+ 8.7	+1.47	+ 7.5	−0.24	−0.03	−0.18	3.53
3151.....	Gr 1618	K6	6.8	220±8	+ 8.5	+1.35	+ 7.5	−0.25	−0.08	−0.09	3.56
2393-C....	YY Gem $\frac{A+B}{2}$	M1	9.6	73±3	+ 8.9	+1.38*	+ 8.1	−0.31	−0.20	+0.09	3.55
4119.....	Lal 25372	M2	8.5	191±8	+ 9.9	+1.42	+ 9.0	−0.39	−0.39	+0.39	3.57
3389.....	Lal 21185	M2	7.6	388±6	+10.5	+1.32	+ 9.4	−0.41	−0.43	+0.45	3.54
1304B.....	o^2 Eri B†	A0	9.48	202±3	+11.0	+0.05†	+10.6	−0.35	−1.66	+2.97	4.02

* The color index is that determined by Hogg (HB 848), reduced to King's scale.

† The color index was assumed from the spectral type.

The relative influence of variations of each of the parameters and the contribution each makes to the observed spectral features may be investigated.

II

3. There would be a number of advantages in having a two-dimensional empirical spectral classification; the operations of the determination of actual values of stellar temperatures and luminosi-

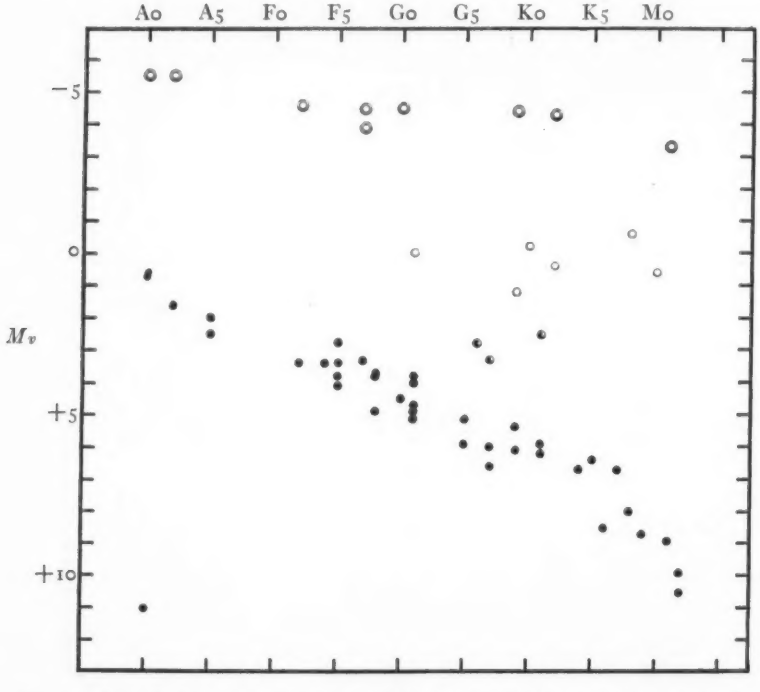

FIG. 1.—Russell diagram for stars in Table 3. Double circles refer to supergiants, open circles to giants, half-filled circles to subgiants, and solid circles to main-sequence stars. The point in the lower left corner refers to the white dwarf o^2 Eridani B.

ties could then be separated from the problem of classifying spectra. Suppose that it had been the custom to publish the actual effective stellar temperature instead of the empirical spectral type. The value of the temperature would then depend not only on the observed spectral criteria but also on the method by which the criteria were discussed in obtaining a numerical value of the temperature.

The argument of the classification, then, would be subject to two sources of error: (1) the error inherent in the criteria themselves and the observational error introduced in their estimation or measurement; and (2) the error introduced in the reduction of the observational data to a temperature scale. The uncertainties introduced in (2) increase unnecessarily the uncertainty in the actual operation of classification. For this reason, and for the sake of the practical

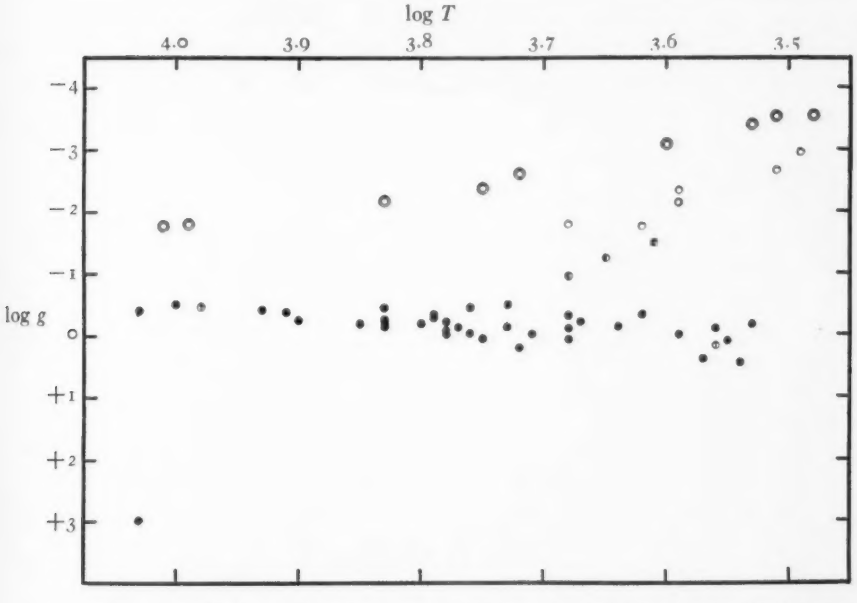

FIG. 2.—Effective temperature-surface gravity diagram for the stars in Table 3. The denotation of the various luminosity groups is similar to Fig. 1; the two bisected circles refer to the eclipsing systems β Aurigae and Castor C.

simplicity of the method, the actual empirical Draper spectral type is a very important and necessary datum.

An actual situation similar to the hypothetical one just outlined exists in the case of the determination of spectroscopic absolute magnitudes. Because of the lack of an intermediate empirical system, it has been the custom to express the vertical spectral classification directly in terms of absolute magnitude. Thus errors, both of a systematic and an accidental nature, are introduced which have nothing to do with the actual classification. As reduction-curves are

changed and improved, the luminosity classification is also changed, although the estimates of line ratios may remain the same. Certain examples of systematic changes are shown in Table 4 for a few bright c-stars, ordinary giants, and main-sequence stars. The absolute magnitudes are taken from successive determinations for the same objects made at Mount Wilson in the period 1917–1935.

TABLE 4

ABSOLUTE MAGNITUDES OF BRIGHT STARS (MOUNT WILSON)

Star	Spec. Mt. W. 1935	Mt. W. 1917	Mt. W. 1921	Mt. W. 1935	M_{trig}	ΔM Mt. W.
ϵ Aurigae	cF2	−0.3	−2.0	−1.7	.....	1.7
α Ursae Minoris	cF7	+0.6	−3.0	−2.2	.....	3.6
γ Cygni	cF7	+1.3	−3.0	−2.1	.....	4.3
ϵ Geminorum	cG8	−1.0	−1.4	−2.1	.....	1.1
ϵ Pegasi	cKo	−0.3	−0.3	−2.3	.....	2.0
Mean	.....	+0.1	−1.9	−2.1	.....	.....
α Aurigae A	G1	+0.3	+0.1	+0.1	0.0*	0.2
β Geminorum	G8	0.8	1.7	0.9	+1.2	0.9
α Bootis	Ko	0.9	1.2	0.2	−0.1	1.0
α Tauri	K5	0.9	1.0	0.0	−0.6	1.0
β Andromedae	Mo	+1.6	+0.5	+0.2	+0.6	1.4
Mean	.....	+0.9	+0.9	+0.3	+0.2	.....
α Canis Minoris	F3	+3.1	+3.2	+3.1	+2.8	0.1
η Cassiopeiae A	F9	5.0	4.3	4.8	4.9	0.7
β Canum Venaticorum	Go	4.4	4.4	4.2	4.5	0.2
τ Ceti	G4	6.2	6.1	5.6	6.0	0.6
σ Draconis	G8	5.4	5.8	5.6	6.1	0.4
61 Cygni A	K6	+7.9	+8.3	+7.7	+8.0	0.6
Mean	.....	+5.3	+5.4	+5.2	+5.4	.....

* M determined from orbit.

It is seen that the mean absolute magnitude of the five bright c-stars has become more than two magnitudes brighter; the luminosity of the ordinary giants has been increased by about half a magnitude, while the main-sequence stars remain approximately unchanged. The changes that have been made are, in the main, changes in the scale of the absolute-magnitude system.

In connection with Table 4 it should be noted that α Bootis is no

longer an anomalous case. The Mount Wilson value for the absolute magnitude in 1921 was +1.2, which is 1.3 mag. fainter than the trigonometric absolute magnitude. In the 1935 list, however, the three first-magnitude stars, β Geminorum, α Bootis, and α Tauri, have all been measured about one magnitude brighter than before; and the spectroscopic luminosities of all three are now in fair agreement with their trigonometric absolute magnitudes.

4. If the various systems of spectroscopic absolute magnitudes differed from each other only by a scale factor, it would be a simple matter to adopt some system as standard, reduce the others to it, and consider the numerical values of the absolute magnitudes as an empirical second dimension to the spectral classification. The transformation of these numerical values into actual absolute magnitudes could then be made an independent operation, which could be revised from time to time as more accurate parallaxes and other data became available. When some of the most extensive systems are compared, however, certain systematic differences are shown which complicate any reduction process. Figures 3 and 4 illustrate such differences in a comparison of Victoria absolute magnitudes with the most recent determinations made at Mount Wilson. All stars common to the two lists in the spectral intervals G5 to G9 and K0 to K3 have been included in the comparison. The remarkable separation of Mount Wilson giants and subgiants is not even suggested by the Victoria results. We are not concerned here with the origin and interpretation of these differences: they are illustrated only to show the practical difficulty of reducing the two systems to a single one.[6]

If a second dimension in the classification is to be introduced, it therefore seems advisable to go back to the actual spectra and to give measures of the value of certain criteria on an arbitrary scale which is defined by type stars. The criteria should satisfy the following requirements: (*a*) they should be as simple as possible and should be usable on spectrograms of rather low dispersion; (*b*) the criteria used for the determination of the Draper type should be insensitive to changes in *g*; (*c*) those used for the vertical classification

[6] Professor Russell is kind enough to allow me to state here that he has also found anomalies in the spectroscopic absolute-magnitude systems.

should be insensitive to changes in Draper spectral type; (*d*) the luminosity criteria should change fairly uniformly with changing absolute magnitude.

The simplest and most sensitive criterion of spectral class among the A stars is the K line. It is relatively insensitive to luminosity

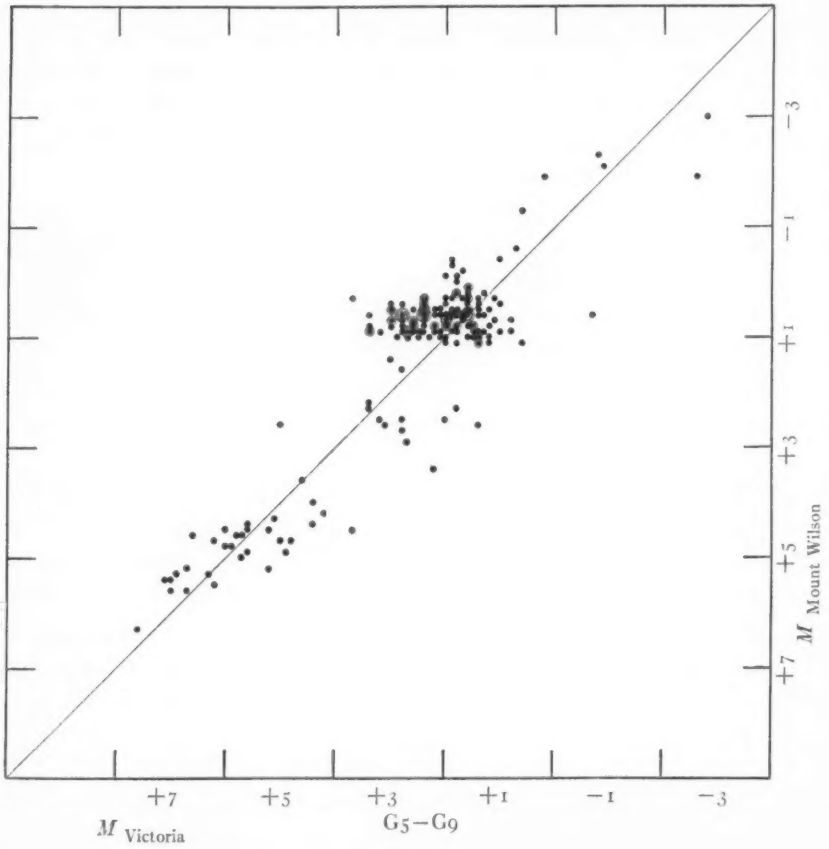

FIG. 3

differences, and in spite of its behavior in a few peculiar objects,[7] it is the most suitable indicator of spectral type in the A and early F stars. Because of their great variation with luminosity, the hydrogen lines are unsuitable for determining spectral types in the A stars; in the spectral range F0 to G5, however, they are much less af-

[7] See *Pub. Yerkes Obs.*, **7**, Part III, 1935.

fected by absolute-magnitude differences, and their rapid decrease in intensity with advancing spectral type makes them especially useful for classification. For types later than G8 the H lines show a strong positive luminosity effect, and they are not suitable for the determination of spectral type in the K and M stars.

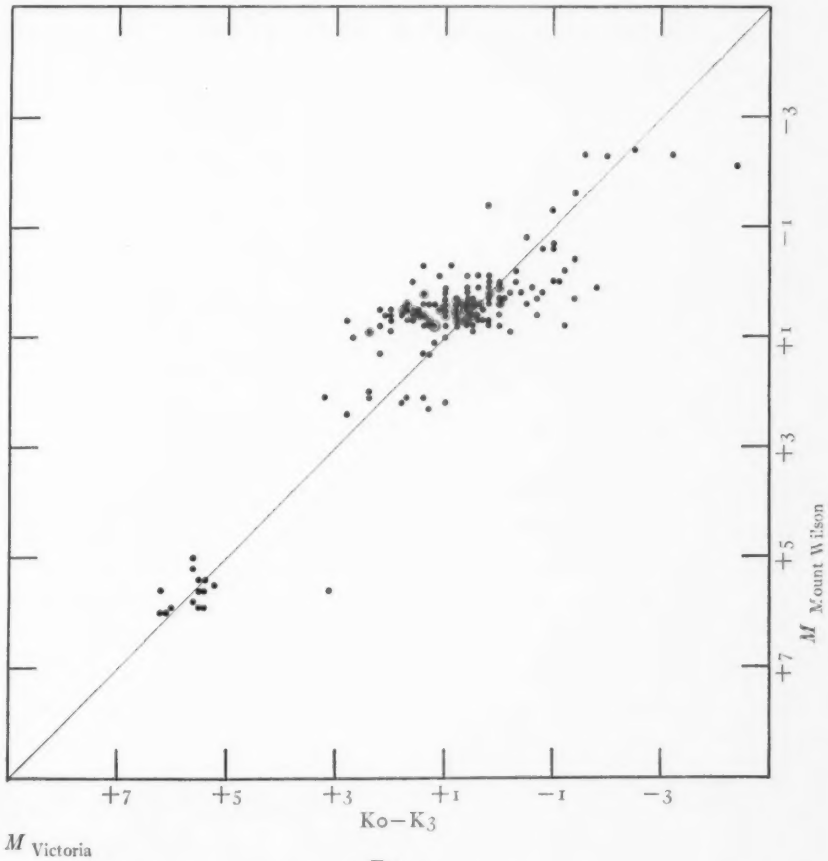

FIG. 4

For slit spectrograms having dispersions of from 60 to 120 A/mm at $H\gamma$ the following have been selected as the simplest and most sensitive criteria of Draper type:

A0 to F5	The intensity of Ca^+ K
F0 to G6	The ratios Fe 4045/$H\delta$ and Ca 4226/$H\gamma$
G4 to K9	The intensity of Ca 4226; G4 to K0, also the intensity of Fe 4045

In the spectral region in which they are used, each criterion is insensitive to changes in luminosity and varies rapidly with spectral type.

A group of stars has been selected to indicate primary standards of spectral type. These stars are listed in Table 5, together with their spectral types as determined from the criteria listed and calibrated by the Victoria system. The primary standards are bright main-sequence stars with large, well-determined trigonometric parallaxes. Reproductions of their spectra are shown in Plate XIX. The spectro-

TABLE 5

Star	Spectrum	m_{vis}	Trig π	M_{vis}
α Lyrae	A0	0.1	$0''.121 \pm 4$	+0.6
β Leonis	A4	2.2	76 5	1.6
ρ Geminorum	F0	4.2	57 6	3.0
1 Orionis	F5	3.3	128 5	3.8
ϵ Persei	G0	4.2	85 4	3.8
μ Cassiopeiae	G5	5.3	130 6	5.9
S 525	G9	5.7	111 7	5.9
S 769	K5	5.9	144 5	6.7
61 Cygni A	K8	5.6	299 3	+8.0

grams were obtained with the 6-inch Moffitt camera attached to the Bruce spectrograph, used with the 40-inch refractor of the Yerkes Observatory. The scale of the original spectra is approximately 110 A/mm at $H\gamma$. The exposures were made on Agfa Super Sensitive Panchromatic cut film and on Eastman Ortho Press plates. The Eastman D-72 formula was used for most of the films; the plates were developed in a special fine-grain developer, the formula of which was worked out by Miss Edith Kellman and the writer. It is unique in that no alkali is used, in spite of the fact that Elon is the only reducing agent present. The gradation obtained is considerably better than that obtained with the commonly used developers of the glycin-paraphenylene-diamine type.

YERKES FINE-GRAIN FORMULA FOR ORTHO PRESS PLATES

Elon or metol	10 gm.
Sodium sulphite (dry)	100 gm.
Water	1000 cc.

Develop 12–18 minutes at 65° F.

PLATE XIX

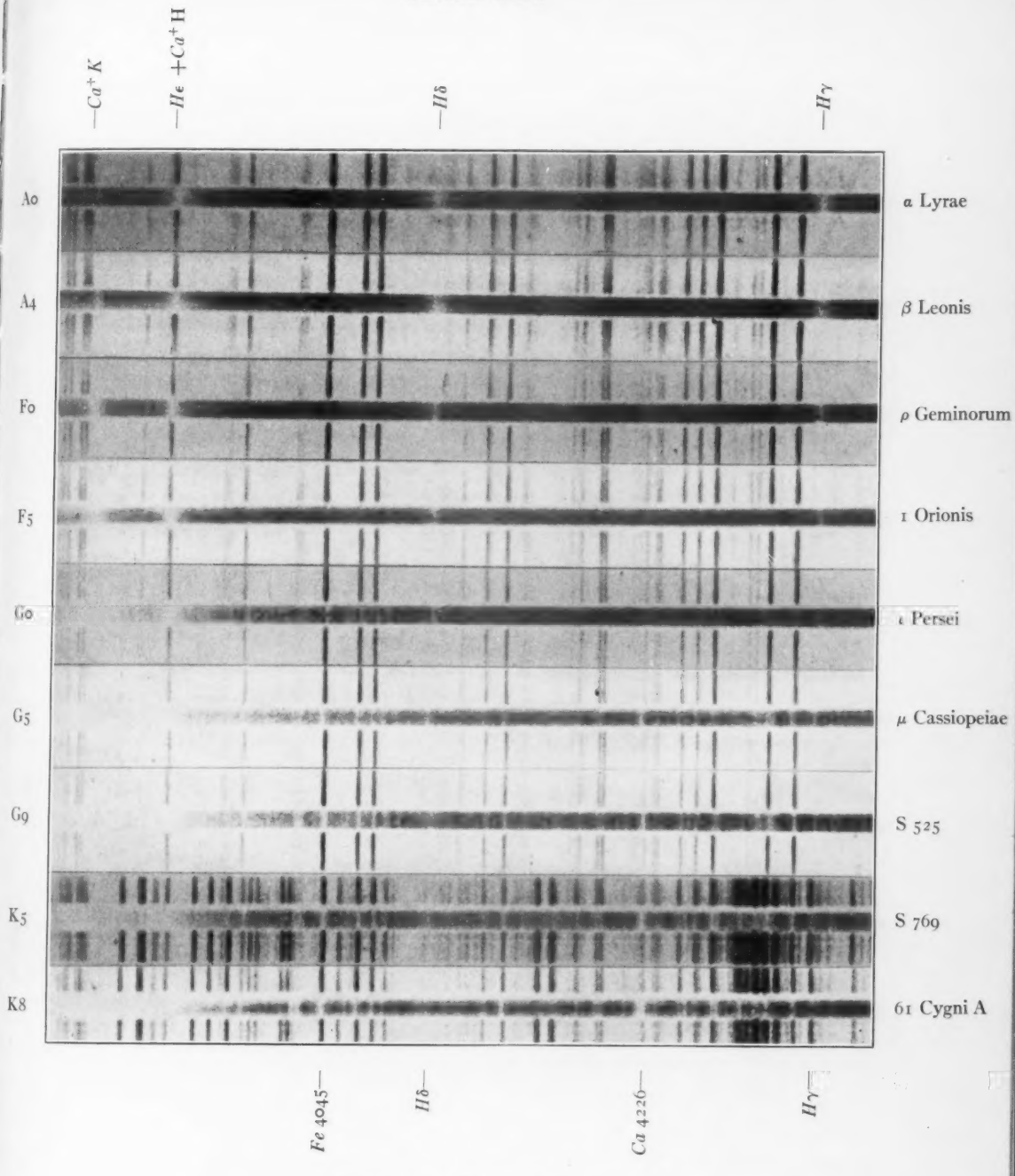

STANDARDS OF SPECTRAL TYPE

CRITERIA

A0–F0 Intensity of K

F0–G5 Ratios 4045/$H\delta$ and 4226/$H\gamma$

G5–K8 Intensity of *Ca* 4226; G5—K0 Intensity of *Fe* 4045

PLATE XX

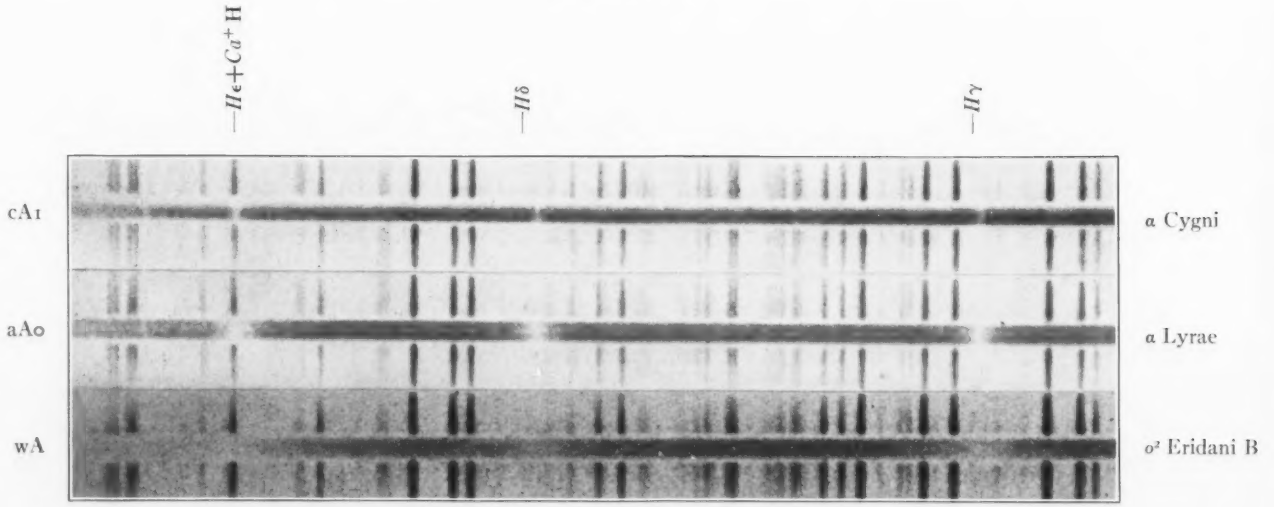

EXTREMES IN LUMINOSITY AMONG THE A STARS

The hydrogen lines are much broader in the main-sequence star α Lyrae than in the supergiant α Cygni, and are broadest of all in the white dwarf o² Eridani B.

The inherent fine grain of Eastman Super-X motion-picture film and the Agfa film mentioned above makes these emulsions especially valuable for spectroscopic work where high speed and minimum graininess are desirable.

5. The criteria selected for determining the second, or luminosity, dimension in the classification are listed in Table 6. The x classes, which correspond to the Draper spectral types, are divided into five groups; within each group the criteria of luminosity, or y class, are the same. The characteristics of each group will now be described in detail:

TABLE 6

Class (x)	Criteria (y)
Ao to A6	Intensity of $H\gamma$ and $H\delta$
A7 to F4	*Fe* 4045 − [*Fe*+*Ti*+ 4172–4], *Ca* 4226 − [*Y*+ *Fe*+ 4177–8], *Fe* 4325 − [*Ti*+ *Sc*+ 4312–5]
F5 to F9	*Fe* 4045 − [*Fe*+ *Ti*+ 4172–4], *Fe* 4045 − *Sr*+ 4077, *Ca* 4226 − [*Y*+ *Fe*+ 4177–8]
Go to G8	*Fe* 4045 − *Sr*+ 4077, *Fe* 4260 − *Sr*+ 4215
G9 to K9	*Fe* 4045 − *Sr*+ 4077, *Fe* 4260 − *Sr*+ 4215, *Fe* 4071 − $H\delta$, *Fe* 4325 − $H\gamma$

Group 1. Ao to A6.—The great increase in intensity in the H lines on passing from the supergiants to the main sequence and from the latter to the white dwarfs is shown in Plate XX, where spectra of α Cygni, α Lyrae, and o^2 Eridani B are reproduced. The problem of determining accurate luminosities of the A stars is essentially a spectrophotometric one; it has been carefully investigated most recently by Öpik and Miss Olmstead,[8] and no attempt will be made here to do more than divide the spectra into three groups: the supergiants, the main-sequence stars, and the white dwarfs. For the luminosity classification the spectral type is prefixed by an "a" for main-sequence stars and a "w" for the white dwarfs; the "c" prefix for the supergiants is retained unchanged.

Group 2. A7 to F4.—This is the earliest group for which line ratios are used. With the dispersion used (110 A/mm at $H\gamma$), the separation of the supergiants from the main sequence can be made

[8] *Harvard Circ.*, No. 380, 1932.

with accuracy, but it is more difficult to distinguish between intermediate giants, such as α Leporis, and the main sequence. For the satisfactory determination of the relative luminosity of the latter two groups, several perfect spectrograms of each object are necessary. There would probably be a considerable gain in accuracy if

TABLE 7

TYPE STARS (Ao TO A6)

α Lyrae	aAo
α Geminorum B	aA1
β Leonis	aA4
σ^2 Eridani B	wA
σ Cygni	cAo
α Cygni	cA1

spectrograms of twice the dispersion employed were used. For this and for all later groups, the y class consists of a prefixed number which is the sum of the individual values of the line differences on an entirely arbitrary scale. This scale is defined by the assigned values of the differences in the type stars.

TABLE 8

TYPE STARS (A7 TO F4)

Star	M_{trig}	x Class	[λ 4045 −λ 4173-4]	[λ 4226 −λ 4177-8]	[λ 4325 −λ 4312-5]	Sum	xy Class
ρ Geminorum	+3.0	Fo	+1	+2	+1:	+4	4 Fo
α Leporis	[−0.8]	Fo	−1	+1	−2	−2	2 Fo
φ Cassiopeiae	[−3.2]	Fo	−3	−3	−3	−9	9 Fo

In Table 8 the column M_{trig} contains, in brackets, the absolute magnitudes for the two giants as determined at the Norman Lockyer Observatory; these spectroscopic absolute magnitudes are included for giants with small trigonometric parallaxes, to show the consistency of the present luminosity classification. For later groups the Victoria absolute magnitudes will be used for this purpose. They were not used for the stars in this group because the absolute magnitude of φ Cassiopeiae was not determined at Victoria. The mean error of determination of a y class from one good plate is about

PLATE XXI

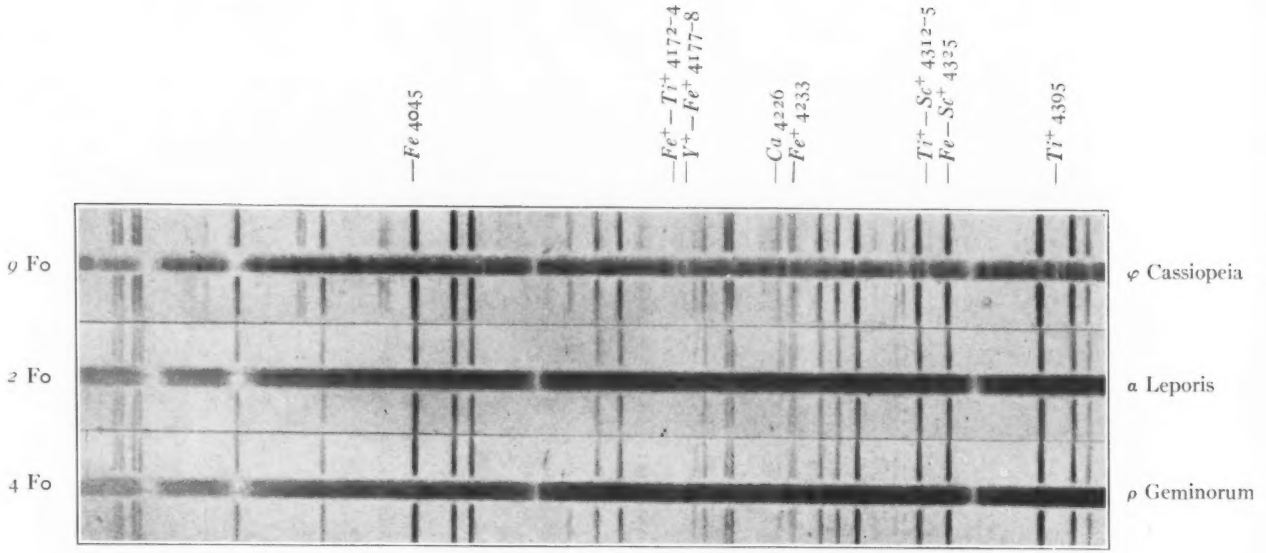

LUMINOSITY EFFECTS AT TYPE Fo

The star φ Cassiopeiae is a supergiant, α Leporis a less luminous giant, and ρ Geminorum a dwarf. The neutral lines of *Fe* and *Ca* are roughly the same in all three stars, while the enhanced lines of *Fe*, *Ti*, and *Y* become stronger with increasing luminosity.

two units for stars of types A7 to F4. Spectra of the three type stars are shown in Plate XXI.

Group 3. F5 to F9.—Two of the luminosity criteria are identical with Group 2. The pair *Fe* 4045 − *Sr*$^+$ 4077 is added at F5; it is not used in earlier types because of the peculiar A2 to Fo dwarfs in which ionized strontium is abnormally strong. The scale for the estimates of this pair is determined in this and in all succeeding groups by defining the difference *Fe* 4045 − *Fe* 4071 = 5 units. The line differences can be estimated on small-scale plates with considerably higher precision than in Group 2. The data on the standard stars are given in Table 9.

TABLE 9

Star	M_{trig}	x Class	[λ 4045 −λ 4077]	[λ 4045− λ 4173–4]	[λ 4226− λ 4177–81]	Sum	xy Class
1 Orionis	+3.8	F5	+3	+3	+2	+8	8 F5
α Persei	[−0.6]	F5	−2	−1	+1	−2	2 F5
γ Cygni	[−3.2]	F5	−4	0	−1	−5	5 F5
η Cassiopeiae A	+4.9	F8	+3	+2	+3	+8	8 F8
ρ Cassiopeiae	[−3.8]	F8	−4	−3	−1	−8	8 F8

Spectra of the stars in Table 9 are reproduced in Plate XXII*A*. The greatest variation with luminosity in the range F5 to F9 is shown by λλ 4045–4077. The probable error of a sum from a single plate is approximately one unit.

Group 4. Go to G8.—The enhanced lines of *Ti*$^+$, *Fe*$^+$, and *Y*$^+$ have become weaker and are no longer suitable for luminosity classification on small-scale plates. The line which is by far the most sensitive to variations in luminosity in the G stars is *Sr*$^+$ 4077. The other resonance line of *Sr*$^+$ at λ 4215 has become strong enough to be estimated with accuracy on the plates used. The standard type stars are listed in Table 10. The probable error of a sum from a single plate is approximately one unit.

Group 5. G9 to K9.—In addition to the two *Sr*$^+$ lines, the pairs *Fe* 4325 − *Hγ* and *Fe* 4071 − *Hδ* are sensitive to luminosity differences, especially between supergiants and ordinary giants. The standard stars are given in Table 11, and the spectra of several of

them are illustrated in Plate XXII *B*. The probable error of a sum on one plate is approximately one unit.

6. From the foregoing it is shown that a rather precise two-dimensional spectral classification of the F5 to K9 stars can be made from slit spectrograms of low dispersion. Spectral types on the

TABLE 10

TYPE STARS (Go TO G8)

Star	M_{trig}	x Class	[λ 4045−λ 4077]	[λ 4260−λ 4215]	Sum	xy Class
ι Persei	+3.8	Go	+6	+1	+7	7 Go
α Aurigae	0.0	G1	+1	−1	0	0 G1
ζ Monocerotis	[−2.3]	Go	−2	−2	−4	4 Go
μ Cassiopeiae	+5.8	G5	+6	+1	+7	7 G5

TABLE 11

Star	M_{trig}	x Class	[λ 4045 −λ 4077]	[λ 4071 −λ 4101]	[λ 4260 −λ 4215]	[λ 4325 −λ 4340]	Sum	xy Class
S 525	+5.9	G9	+7	+3	+2	+4	+16	16 G9
β Aquilae	+3.3	G9	+6	0	+1	+3	+10	10 G9
β Geminorum	+1.2	G9	+4	+2	−1	+3	+ 8	8 G9
ε Geminorum	[−1.9]	G9	−1	−3	−3	−1	− 8	8 G9
o^2 Eridani A	+6.0	K1	+8	+3	+2	+4	+17	17 K1
γ Cephei	+2.5	Ko	+7	+3	−1	+4	+13	13 Ko
α Bootis	−0.1	Ko	+2	0	0	+3	+ 5	5 Ko
ζ Cephei	[−2.0]	Ko	0	−2	−4	−1	− 7	7 Ko
61 Cygni A	+8.0	K8	+9	+4	+3	+5	+21	21 K8
α Tauri	−0.6	K8	+3	+4	0	+3	+10	10 K8

Draper system can be determined with high accuracy; the mean error of a determination is about one-tenth of a class, except in the range A7 to F4, where it is somewhat higher. The stars of types Ao to F4 may be divided, without ambiguity, into three luminosity groups: the supergiants, the main-sequence stars, and the white dwarfs. For types later than F4 the luminosity classification is of considerably higher accuracy, and it is possible to determine accurate spectroscopic absolute magnitudes.

The importance in the extension of the line-ratio method to

PLATE XXII *A*

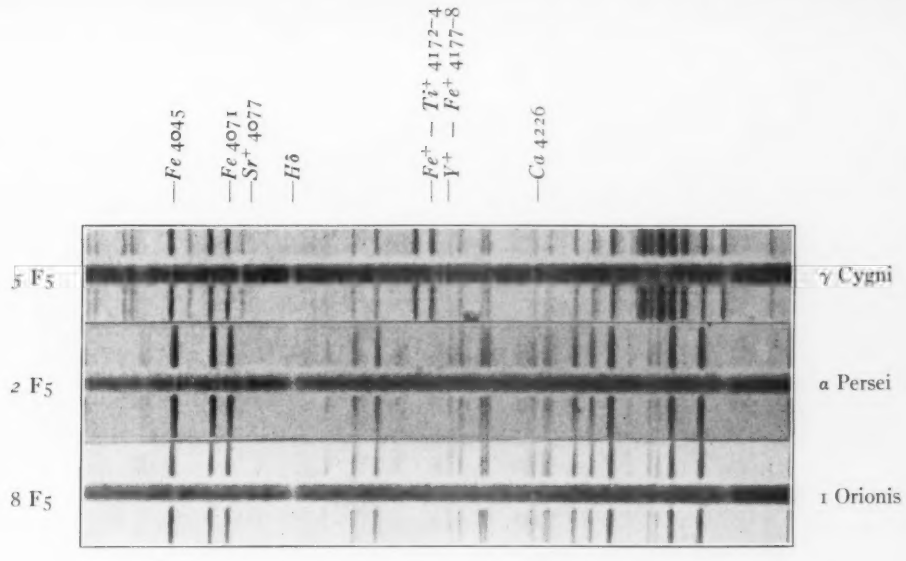

LUMINOSITY EFFECTS AT TYPE F5

The most sensitive line is Sr^+ 4077. It is fainter than *Fe* 4045 in the dwarf 1 Orionis, and becomes stronger than λ 4045 in the giant α Persei; in the supergiant γ Cygni it is almost as strong as *Hδ*.

PLATE XXII *B*

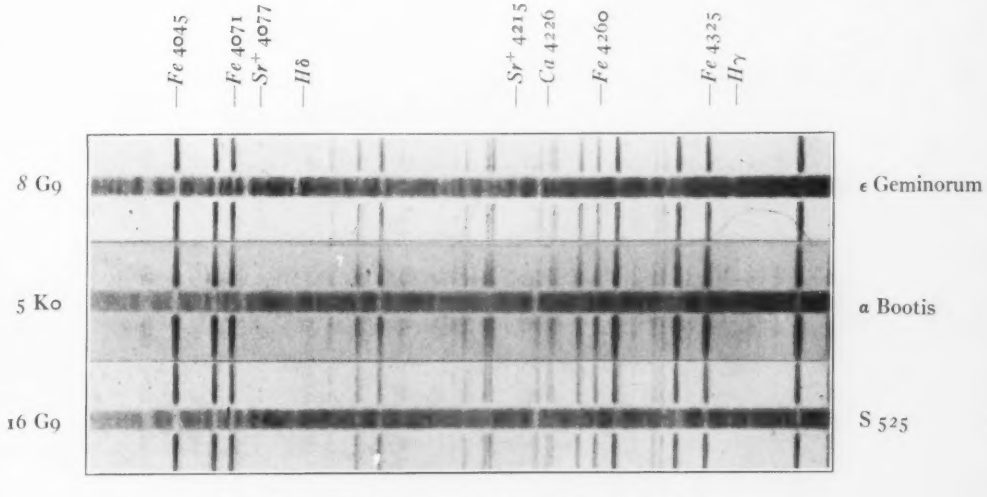

LUMINOSITY EFFECTS IN THE NEIGHBORHOOD OF K0

The most sensitive lines are Sr^+ 4077 and *Hδ*; a comparison with the *Fe* arc lines at λ 4045 and λ 4071 shows that in the supergiant ε Geminorum Sr^+ 4077 is slightly stronger than *Fe* 4045; in the giant α Bootis it is intermediate in intensity between λ 4045 and λ 4071, while in the dwarf S 525 it is weaker than λ 4071. A comparison of *Hδ* with *Fe* 4071 shows a similar sequence in variation.

spectrograms of low dispersion lies in the possibility of observing large numbers of faint stars. The spectrogram of the white dwarf o^2 Eridani B (visual magnitude 9.5), shown in Plate XX, required an exposure time of 20 minutes under fairly good observing conditions with the 40-inch refractor. With the largest reflectors, spectra of equivalent dispersion could be obtained with considerably shorter exposure times, and the number of stars for which luminosities and distances could be determined is very great.

In a later paper the method developed here will be applied to a number of stars which will serve to define accurately the two-dimensional classification system.[9]

I wish to acknowledge the aid which a conversation with Dr. H. N. Russell gave me in formulating the classification scheme outlined in the second part of this paper. Dr. Bengt Strömgren has been kind enough to read the manuscript, and I am indebted to Dr. G. P. Kuiper for the values of the masses of the system o^2 Eridani BC. A number of the spectrograms used in the discussion were obtained by Dr. P. C. Keenan and Mr. G. W. Wares. The computations in Part I and the reproductions of standard spectra were made by Miss Edith Kellman.

YERKES OBSERVATORY
March 9, 1937

[9] I am indebted to Dr. Russell for stressing the importance of using a large number of stars as standards of spectral type.

NOTES

NOTE ON THE ORBIT OF κ PEGASI

When redetermining the elements of the visual and spectroscopic orbits of κ Pegasi,[1] the writer assumed, with Henroteau, that the published position angles of the visual pair actually refer to the brighter component as origin and that this brighter component is the spectroscopic binary, and he thus derived a positive value for the sign of the inclination. Drs. van den Bos and Finsen point out, however, that the visual difference in magnitude is vanishingly small; hence the position angle, as well as the sign of the inclination, is still ambiguous.

It occurred to the writer that a solution might be found in the following way: Since Henroteau's spectrograms show the lines due to the other visual component only occasionally, and then faintly, we may assume that this other visual component, *B*, is redder than the spectroscopic binary, *A*. There happen to be available two excellent series of parallax plates, taken at about the time when the visual pair had its maximum separation. Two "blue" plates were taken at the Allegheny Observatory on June 27 and July 4, 1917, while four "yellow" plates were obtained at the McCormick Observatory on June 29 and July 1, 1917. The calculated position angle and separation at that time were 115° and 0".26, respectively.

The inclination of the orbit was determined as +109°, on the assumption that this angle of 115° indicates the position of the yellower star, *B*, relative to the bluer spectroscopic binary, *A*. If this is actually the case, then at that time *A* preceded *B* by about 0".23, and the right ascension of the blue image should be *less* than that of the yellow image. I am greatly indebted to Dr. F. C. Jordan, of the Allegheny Observatory, and Dr. S. A. Mitchell, of the Leander McCormick Observatory, for their kindness in sending me the original plates for measurement, and to Dr. G. Van Biesbroeck for his will-

[1] *Ap. J.*, **79**, 449, 1934.

ingness to measure the Allegheny plates, which proved to be too large for us to handle.

The result of measurement and calculation gives:

Right Ascension: Yellow minus Blue = + 0".052 ± 0".029 (m.e.) .

The uncertainty was calculated from the internal discordances only, which indicated a mean error in the adopted place for the mean of each series of 0".020. The actual error of the difference may well be larger, and the foregoing result should not be considered as conclusive. In so far as it means anything, it confirms the assumptions made before and indicates that the sign of the inclination is positive. Perhaps further confirmation may be obtained by visual observers using large telescopes, by observing the star through a yellow and a blue filter and noting the position of the brighter star in each case. This should remove all doubt as to the quadrant.

W. J. LUYTEN

MINNEAPOLIS, MINNESOTA
March 29, 1937

REVIEWS

Galaktischer Atlas. By K. F. BOTTLINGER. Berlin: Julius Springer, 1937. Pp. 8. Pls. VIII. Rm. 15.

This atlas in galactic co-ordinates contains all stars brighter than magnitude 5.5, and a number of open clusters, globular clusters, planetary nebulae, bright diffuse nebulae, and dark nebulae. The stars are given with their spectra, and those which have no Greek-letter designations are indicated by their Flamsteed numbers or BD numbers. The limits of the constellations are those adopted by the International Astronomical Union in 1930. A short table permits the conversion of equatorial co-ordinates into galactic co-ordinates. The atlas was started by Dr. Bottlinger at the Berlin-Babelsberg Observatory, and was completed, after his death, by Miss Irmgard Beck. It will be found convenient for a rapid orientation with respect to the Milky Way. The outlines of the latter are indicated roughly by the isophotes of Hopmann corresponding to a step of 1.7 mag. For many current investigations it would have been useful to show the zone of avoidance of extragalactic nebulae. However, since the latter is not equally well determined for all parts of the Milky Way, it is probably best to depend upon a photometrically determined isophote. The symbols used for the stars do not give prominence to those of greater brightness, and the atlas is not intended for rapid identification of stars in the sky. Because of the selection of the co-ordinates, the configurations of the stars are inverted with respect to their appearance in the sky.

O. STRUVE

INDEX TO VOLUME 85

SUBJECTS

INDEX TO VOLUME 85

AUTHORS